CHESTER

Compressed Heat Energy Storage for Energy from Renewable sources

Detailed design of the ECT engine-pump laboratory prototype

PROJECT	**CHESTER**
PROJECT NO.	**764042**
DELIVERABLE NO.	**3.5**
DOCUMENT VERSION	**V2**
DOCUMENT PREPARATION DATE	**19/09/2019**
RESPONSIBILE PARTNER	**ECT**
DISSEMINATION LEVEL	**Public**

Type of Deliverable		
R	Document, Report	**X**
DEM	Demonstrator, pilot, prototype	
DEC	Websites, patent fillings, videos, etc.	
OTHER		
ETHICS	Ethics requirements	
ORDP	Open Research Data Pilot	

This project has received funding from the European Union's Horizon 2020 research and innovation programme under grant agreement No. 764042.

EC Grant Agreement	No.764042
Project Acronym	CHESTER
Project Title	Compressed Heat Energy Storage for Energy from Renewable sources
Programme	HORIZON 2020
Start Date of Project	01-04-2018
Duration	48 Months

Financial/Administrative Coordinator	
Project Coordinator Organization Name	TECNALIA
Address	Parque Tecnológico de Bizkaia C/Astondo, Edificio 700 (Spain)
Phone Numbers	+34 946 430 850
E-mail Address	nora.fernandez@tecnalia.com
Project web-site	www.chester-project.eu

Version Management			
Filename		D3.5 Detailed design of the ECT engine-pump laboratory prototype	
Author(s)		Alexander Kronberg	
Reviewed by		Donal Cotter	
Approved by		Felipe Trebilcock	
Revision No.	**Date**	**Author**	**Modification description**
RV 1	16-09-2019	A. Kronberg	First version
RV 2	18-09-2019	F. Trebilcock	WP3 leader first review with comments
RV 3	19-09-2019	A. Kronberg	High Quality Deliverable version available
RV 4	23-09-2019	Donal Cotter	Reviewed with minor corrections
RV 5	25-09-2019	A. Kronberg	Corrected according to the review
RV 6	27-09-2019	Donal Cotter	Review completed
RV 7	27-09-2019	N. Fernandez	Final formatting

Contents

List of Figures

List of Tables

Glossary, abbreviations and acronyms

A	area (m²)
d	diameter (m)
f	frequency (Hz)
h	specific enthalpy (J/kg)
H	enthalpy (J)
k	overall heat transfer coefficient (W/(m²K))
L	length (m)
m	mass (kg)
$\dot{M}$	mass flow rate (kg/s)
p	pressure (bar)
P	power (W)
Q	heat (J)
$\dot{Q}$	heat flow rate (W)
t	time (s)
T	temperature (K)
u	specific internal energy (J/kg)
U	internal energy (J)
V	volume (m³)
V_0	swept volume (m³)
V_{C0}	cold dead volume (m³)
V_{H0}	hot dead volume (m³)
w	flow velocity (m/s)
w_{spec}	specific work per cycle (J/m³)
W	work (J)

Greek symbols

ε_R	regenerator effectiveness
η	energy conversion efficiency
η_R	overall regeneration efficiency
ξ	friction factor
ρ	density (kg/m³)

Indices

$1-4$	state points in thermodynamic cycle
$+$	added
act	actual
av	average
C	Cold
$C+$	additional cooling
$char$	characteristic
cy	Cycle
Del	delivering
fr	friction
H	Hot
$H+$	additional heating
$high$	high pressure
i	related to discrete element *i*
in	flowing in
low	low pressure
$high$	high pressure
R	regenerator/recuperator
rel	Relative
Rec	Receiving
Res	Residence
$shift$	Shifted
tot	Total
x	related to element *x*

1. Introduction

1.1. Executive Summary

The CHEST system converts the stored renewable energy to electric power and at the same time, it consumes electricity for its operation. The high-pressure ORC pump is the main electricity consumer. In the most efficient ORC operation mode the electricity consumption of the CHEST system is about 15% of the produced electricity. In part-load regimes this percentage can reach values up to 30 % of useful ORC power.

For improvement of the overall energy efficiency of the CHEST system it would be beneficial to use the available heat sources (thermal storage or seasonable thermal energy storage) for pumping operations. However, modern heat engines (internal combustion, Rankine cycle, ORC…) are not economic enough for effective conversion of middle and low-temperature heat to usable energy.

To resolve the technical problems of the current low-grade heat conversion a concept of "isobaric expansion" (IE) engine (also known as Up-Therm, Encontech, ECT engines) is proposed (Glushenkov and Kronberg, 2012 [1]; Glushenkov et al., 2014 [2]; Glushenkov et al., 2018 [3]). Isobaric expansion process of these types of engines is an alternative to near isentropic gas/vapour expansion accompanied by a pressure decrease typical of all state-of-the-art heat engines. The new working cycle of the IE engine is performed with a dense working fluid which is liquid at the low cycle temperature and gas or supercritical fluid at the high cycle temperature.

Elimination of the expansion stage associated with useful work means that compared to ORC systems, the most critical and expensive parts (turbine, screw expander, etc.), as well as pump, are not needed anymore. In addition, usable energy is provided in a very convenient hydraulic form. The proposed system does not suffer from typical technical problems of well-known thermal energy driven systems: sealing, lubrication and wear. The system is noiseless, can be fully balanced and has a very simple, reliable and inexpensive design.

The IE engine can perform all the known engine operations, in line with basic volumetric compressor and pump operations. Such compressors and pumps can use arbitrary heat sources with temperature above 70 ^{0}C and do not need lubrication.

The IE engines are particularly promising and favourable for the CHEST system. By applying the ECT engine the available heat sources (including low-value heat, below 100 ^{0}C) of the CHEST system can be effectively used to drive directly, without electricity use and pertinent electric equipment, all pumps of the CHEST system, while also generating electricity. In particular, the novel IE low-temperature heat driven engine-pump will increase the net electric efficiency of ORCs by at least 5% (up to 30%) by replacing high pressure conventional refrigerant pump. In addition to the improvement of system´s energy efficiency, a reduction of the capital cost can be foreseen, because of both the elimination of electricity consuming equipment and due to the replacement of bulky pumps (the engine operates as a pump).

The IE engines have shown significant potential. Technical and economic feasibility have been demonstrated at the power range of 5-20 W and heat source temperature above 80 ^{0}C.

The goal of Task 3.4 within the CHESTER project is to develop further this promising technology for applications relevant for the CHEST system. In the course of the project an IE engine-pump of about 1 kW output and operated at heat source temperature of >80 ^{0}C will be designed, built and tested. Technical simplicity and scalability are important requirements to this novel machine.

Eventually an assessment of the applicability of this novel heat engine for other potential applications related to low temperature heat revalorization will be performed.

Deliverable D3.5 provides:

- basic information on the novel heat engines and their application as pumps.
- developed theoretical background for the analysis and design of the IE engines and the results of the engine modelling.
- novel engine-pump design, its production drawings and an assembly of the built engine-pump.

1.2. Purpose and Scope

The purpose and scope of this deliverable is to investigate theoretically the novel energy conversion technology and provide an IE engine design that can be used as the heat driven ORC´s high-pressure pump (refrigerant pump). Deliverable D3.5 is related to Tasks 3.4.1 and 3.4.2 of the CHESTER project. The following main outcomes are presented in this report under these tasks.

Task 3.4.1 ECT Engine thermodynamic analysis and modelling.

- Thermodynamic model of regenerative displacer-type heat engines suitable for arbitrary working fluids and arbitrary engine cycles.
- Thermodynamic limits on the heat regeneration in case of non-ideal fluids.
- Calculations of the engine-pump thermal efficiency and specific power for different working fluids at different temperatures of the heat source and pressure heads.
- Modelling of heat exchangers (heater, cooler and regenerator) of the IE engines for the determination the design parameters providing the required power of the ORC high-pressure pump (Task 3.3.1).
- Working fluids of the engine that is suitable for operation at conditions pertinent to high pressure ORC pump.

Task 3.4.2 ECT Engine-pump design and manufacturing.

- Production drawings of the engine.
- Production drawings of the pressure converting units.
- Engine-pump standard components.
- Engine-pump assembly and test set-up.

Originally the IE engine was supposed to be used as the ORC high pressure heat driven pump. However, at the initial stages of the CHESTER project a discussion between the project partners regarding application of the IE engine was held.

It was decided to completely de-couple the ECT engine-pump development from the Chester prototype in view of the engine universality. For instance, the IE engine can replace other electric driven pumps of the CHESTER system, to generate electricity from the available heat sources in parallel to or instead of the ORC. This new approach gives ECT full flexibility to define the IE engine at the most appropriate conditions (specifications), i.e. to select the best IE engine-pump type, define the working temperatures for the heat source and sink, working fluid, etc.

The situation was exposed to the Chester coordination team and approved from their side. Also, the Grant Agreement document was reviewed in more detail and it was confirmed that there was no further conflict in proceeding with this modification (new approach within Task 3.4).

1.3. Methodology

The research plan covers this radically new IE energy conversion technology starting from the thermodynamic fundamentals to the experimental validation of the whole engine-pump. The first steps are for scientific underpinning of the technology, whereas the last ones for proof-of-principle and full technology assessment. The research comprises of a combination of interrelated experimental and theoretical studies of the thermodynamics, heat transfer, fluid dynamics, technical solutions for the main components, and whole IE engine-pump performance. During the project a heat driven pump with useful power of about 1 kW will be made available for the demonstration.

The methodology will be theoretical (modelling and simulation of components behavior; thermal, mechanical, fluid-mechanical and cost aspects will be considered) and experimental (building and testing of components and the whole system). The research will consist of designing a low-temperature heat driven pump and a combination of experimental and theoretical studies of its main components (heater, regenerator, and cooler) and IE engine-pump system.

The available software and experimental facilities and new modelling programs (to be developed) and system components (to be designed, such as engine heater, regenerator, and cooler) will be used. These studies will focus on the improvement of design of the main components, determination of an optimal working fluid and eventually achieving highest energy conversion efficiency at minimal cost.

1.4. Structure of the document

The report is divided in four chapters of which the first one is Introduction.

- Chapter two provides basic information on the novel heat engines and their application as a pump.
- Chapter three provides a theoretical background for the analysis and design of the IE engines and the results of the engine modelling. The results include selection of working fluid for the IE engine-pump and guidelines for design of the engine heat exchangers.
- Finally, chapter four describes different engine concepts and provides production drawings of the engine-pump parts that have been designed. Finally, standard components and final assembly of the engine-pump are presented.

1.5. Relations with other deliverables

In the preparation of this document, information from all the existent deliverables in WP2 and WP3 was considered. From WP2, information regarding the CHEST system boundary conditions was used, while from WP3, deliverables D3.1 to D3.4 were used in order to understand the expected interaction of the IE engine-pump with other components of the CHEST prototype.

The results from this deliverable will serve as the bases for the preparation of future deliverables related to the development of the IE engine-pump, namely deliverable D3.9 and deliverable D3.15. On the other hand, deliverable D3.5 might also provide referential information to deliverable D3.11, related to the extended performance maps for the individual technologies.

2. Isobaric expansion engines

2.1. Basic principle

The IE engine, as with other heat engines, uses temperature difference between a heater and cooler to generate mechanical energy through a working fluid. Alternative heating and cooling of the working fluid results in its expansion and compression with the overall positive work. All that is needed is a source of heat and a source of cold and where that heat comes from is irrelevant to the heat engine. The main differences when comparing this technology to other know technologies is the use of dense working fluids, novel compression-expansion cycles, hydraulic power as an output and a new heat engine design.

The idea of a dense working fluid, which is liquid at the low cycle temperature and gas or supercritical fluid at the highest cycle temperature, appeared due to several fundamental and technological reasons listed below.

- Liquids, if not near the supercritical conditions, are almost incompressible, and therefore decrease remarkably the negative impact of dead volumes in the cold space and regenerator. Only this effect may double both the thermal efficiency and power density of the engine. Malone was probably the first who explored incompressibility of water in the cold space in his Hot-Water engine (Sier, 2007 [4]). Later, the Thermo-Electron Corporation developed the 'tidal regenerator engine' with a condensing working fluid (Walker, 1980 [5]).
- Sealing of liquid to prevent working fluid leakage is much easier than that of gases especially such as hydrogen and helium, which are often used in Stirling engines.
- The pressure difference in the compression and the expansion steps with a liquid exhibiting phase transition or with supercritical fluids can be very high, up to several hundred bar. Accordingly, a very high-power density can be obtained, which makes the engine compact. For example, CO_2 is one of the promising working fluids; if CO_2 at 20 ^{0}C and 100 bar is heated up to 300 ^{0}C, its volume will increase 5 times at 200 bar. So, 100 bar pressure difference and 5-fold expansion will be produced by 280 ^{0}C heating and resulting in 40 J/g work - several orders of magnitude higher than that of conventional energy absorption materials (Chen et al. 2014 [6]).
- Another practical consequence of the very high-pressure differences is that no high frequency and accordingly high rubbing speed of moving parts is necessary to have high power density. This facilitates elimination of wear and increases lifetime of the engine.
- All rubbing and sealed parts can be in the cold part of the engine filled with liquid, which has better lubricating and frictional heat rejecting ability. Moreover, liquid working fluid permits the use of hydrostatic fluid bearings eliminating any rubbing friction and wear.
- Liquid working fluid improves the heat exchange significantly compared to gas working fluid (as thermal conductivity of liquids is much higher than that of gases, e.g. at 25 ^{0}C for nitrogen it is 0.024 W/(m K) whereas for water - 0.58 W/(m K), i.e. almost 25 times higher).
- Liquid working fluid makes the converter much safer since the operation volume of gas/vapour phase is smaller, whereas out of operation a high-pressure gas phase can be absent.
- Real gas effects in the critical region during compression process, although theoretically detrimental in ideal cycles, give important efficiency gains in real Stirling cycles mainly

owing to reduced compression work (Angelino and Invernizzi, 2000 [7]). Due to the low compressibility (several times lower than that of ideal gas) the compression work will be much smaller.

- Liquid working fluid permits using both recuperative and regenerative regenerators in contrary to solely regenerative regenerator for the conventional Stirling engines.
- Liquid working fluids make it possible to use much lower temperature of heat sources compared with the conventional Stirling engines.
- With liquid working fluids hydraulic power output is a logical technical solution: energy of the working fluid is transmitted to hydraulic oil through a diaphragm or to the liquid working fluid itself. The hydraulic power output provides greater design flexibility and the engine can be used for multiple purposes and easily balanced. The generated hydraulic power can be transmitted over long distances either from multiple engines to one end-user or from a single engine to multiple end-users.

These advantages in combination with a unique cycle permit development a very simple, inexpensive, robust and safe design.

During the development of the IE engine-pump for CHEST system two concepts of engines were proposed and studied. The first concept is based on significant changes to the original concepts of the Worthington steam pump and the second on modification of the Bush thermo-compressor. These two types of IE engines are described in the recent publication by *Glushenkov et al. 2018* [3].

In the current report only the Bush thermo-compressor based concept is considered. However, according to thermodynamic simulations for a number of selected working fluids and operating conditions, the Worthington based concept could be of interest for low-temperature applications, below 80 ^{0}C and can also be used for the CHEST system.

Basic principle of operation of the externally (forcedly) actuated IE engine based on the Bush thermo-compressor is shown in the Figure 1.

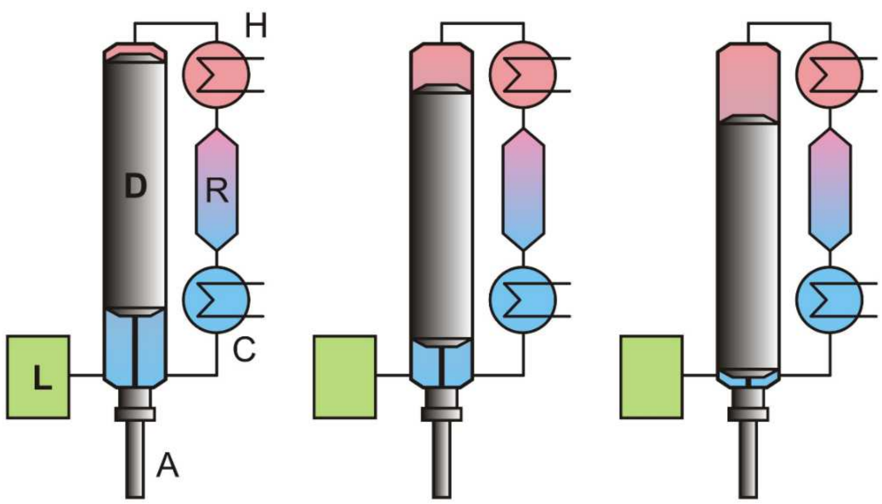

Figure 1: Externally actuated IE engine: basic principle.

The engine is filled with a liquid working fluid. In operation, a linear actuator (A) moves the displacer piston (D) up and down with a relatively low frequency of about 1 Hz. Moving down, the displacer displaces 5-30% (depending on pressure and temperature) of liquid working fluid from the lower, cold part of the cylinder (shown in blue) through the cooler (C), regenerator (R) and heater (H) to the upper, hot part (shown in rose). Flowing through the regenerator and heater, these 5-30% of working fluid heats up and turns into vapour; pressure in the cylinder rises and the rest 70-95% of liquid working fluid is forced out of the cylinder to an engine load (L), e.g. moving a piston or diaphragm.

When the displacer moves up it displaces the vapour of the working fluid from the upper, hot part of the cylinder back to the cold, lower part. Flowing through the regenerator and cooler, the vapour turns back into liquid. As pressure in the cylinder drops down, and all the displaced liquid returns from the load to the engine cylinder.

The working fluids used (refrigerants, light hydrocarbons and their mixtures) permit the engine to operate from low grade heat sources (70 – 100 ^{0}C).

In contrast to all conventional heat engines (piston engines, gas and steam turbines), which have (rotary) shaft power output, IE engines have hydraulic output. This makes the IE engine very versatile with respect to different applications.

2.2. Engine applications

The engine can perform all operations like other heat engines. Volumetric compressors and pumps have simple operation and logical loads, and the engine itself operates as a pump or compressor. One out of many examples is shown in the Figure 2.

They contain a differential piston reciprocating inside a differential cylinder, which is a simple design with no transmission or crank gear etc. The differential piston (a combination of two pistons with different diameters) makes it possible to convert the pressure difference generated by the IE engine to any convenient combinations of initial and discharge pressures. Such compressors and pumps do not need lubrication.

They can compress also vapours; in this case the whole installation can be easily turned into different variations of thermally driven heat pump or cooling/refrigeration unit.

Energy from the liquid/gas flows generated by such an installation can be converted to shaft power (rotary motion) and also to electricity by means of well-known mass-market hydraulic or pneumatic motors. In this case the installation is turned into a heat-driven electric generator, which differs from conventional known generators it can also produce electricity using a very low-grade heat (geothermal, waste, etc.).

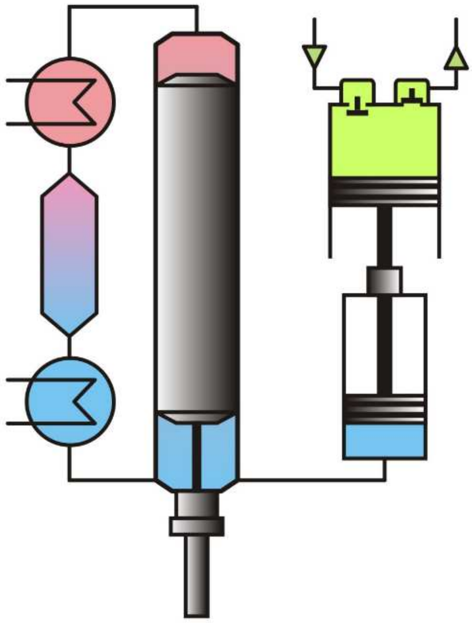

Figure 2: Externally actuated IE engine as a pump/compressor.

Hydraulic output from IE engines permits integration with other non-conventional technologies, such as piezoelectric, electrochemical etc. This IE engine feature opens great opportunities for innovative electricity generation methods.

One of most promising methods of electricity generation with IE engines is a liquid metal magneto-hydrodynamic generator (LMMHD), see Figure 3. If a liquid metal (for instance, a very cheap alloy of Na-K, liquid up to minus 120 °C) flows inside a duct across a magnetic field (B), electric current is generated between two wall-electrodes shown in violet. Such a method was always recognized as a cheap, simple, energy dense technology of power generation. But it needed a technology, directly converting heat to the liquid metal flow (which did not exist). As a result, this method was abandoned.

Current research using IE technology may now offer a practical solution to previous thermal conversion issues, as LMMHD ideally combines with IE engines. An example is shown in illustration Figure 4.

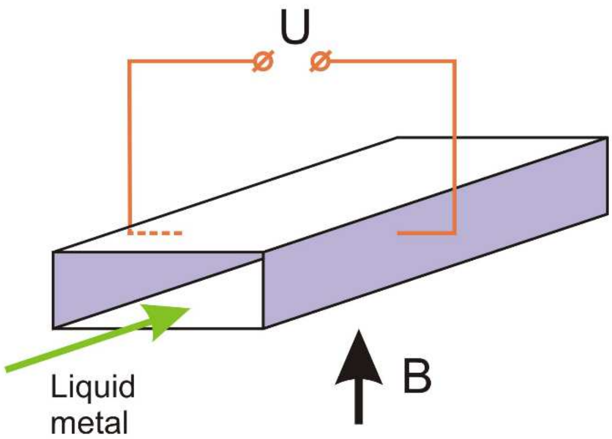

Figure 3: Liquid metal magneto-hydrodynamic generator.

There are two IE engines with LMMHD in between. Each engine is provided with a diaphragm unit (DU) which has a thin polymer or metal diaphragm transmitting pressure of the working fluid to the liquid metal and back. Both engines operate in counter-phase. The liquid metal flows through LMMHD back and forth generating electric current using heat from any source or grade. This is a good example how two unconventional technologies may effectively strengthen each other.

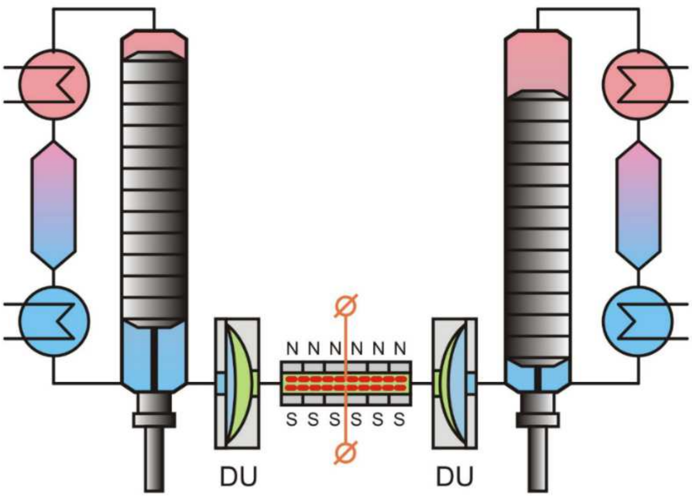

Figure 4: Unconventional application of the IE engine for electricity generation.

2.3. Self-driven concept

The displacer of the IE engine can be driven by an external actuator as shown in Figure 1, Figure 2 and Figure 4. However, there are many ways to make the engines self-driven. All of them are based on the creation of a pressure drop over the displacer piston. One of many examples is shown in Figure 5.

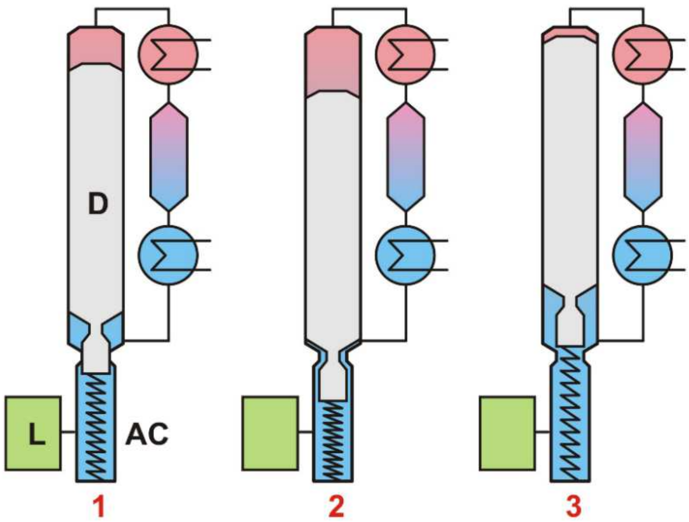

Figure 5: IE engine with self-driven displacer.

In this case the engine has a second, auxiliary cylinder (AC) with a spring inside. In addition, the displacer (D) has a more complicated design: the lower end is provided with a spool valve. This valve communicates the main and auxiliary cylinders when the displacer is in upper and lower position (top and bottom dead centre 2 and 3) and separates the cylinder in all other positions of the displacer. The operation of the engine has a lot in common with the outlined above operation of forcedly actuated engine.

Initially, the displacer is held by the spring in the middle position (1); both the cylinders are disconnected. When heat is supplied, the pressure in the main cylinder rises overcomes the force of the spring and moves the displacer down. Moving down, the displacer forces the working fluid from the cold (blue) lower part of the main cylinder through the regenerator and heater to the hot (rose) upper part. The pressure rises, moving the displacer down further and compresses the spring. The liquid from the auxiliary cylinder is displaced to a load (L). At the end of this down stroke (2) the main and auxiliary cylinders are connected by the spool valve. High-pressure liquid from the main cylinder goes to the auxiliary cylinder and then to the load (L). The pressures in the main and auxiliary cylinders equalize and the spring pushes the displacer up. The spool valve disconnects the main and auxiliary cylinder. Moving up, the displacer displaces vapour from the upper hot part of the main cylinder through the regenerator and cooler to the cold lower part. Pressure in the main cylinder drops down and becomes lower than pressure in the auxiliary cylinder. As a result, pressure in the auxiliary cylinder lifts the displacer up and expands the spring. In the upper position (3) of the displacer, the spool valve then activates the main and auxiliary cylinders. The liquid working fluid flows from the load through to the auxiliary cylinder to the main one. The pressures in the main and auxiliary cylinders equalize and the spring pushes the displacer down. The spool valve disconnects the main and auxiliary cylinder and the cycle repeats itself.

3. ECT engine thermodynamic analysis and modelling

3.1. Introduction

Displacer-type regenerative heat engines ([5], [8], [9] & [10]) represent an alternative to Rankine cycle (RC) and Organic Rankine cycle (ORC) engines as well as to internal combustion engines. Among their greatest advantages is flexibility with regard to the type and grade of the heat source, low emission and often quiet or even noiseless operation [11]. While RC and ORC plants are the dominant technology in large-scale heat conversion [12], their technical complexity makes them too expensive for mini-scale (< 50 kW) and micro-scale (< 1 kW) applications and low-grade heat conversion ([13], [14]). Regenerative piston-type engines, such as Stirling engines, were often thought to be an ideal solution for this type of operation ([15], [16]). Difficulties in the technical realisation, however, hindered significant commercial success of these machines. Lubrication of rubbing parts, high-pressure and high-temperature gas sealing as well as the negative effect of inevitable dead volumes on the efficiency are among the most serious disadvantages of Stirling engines ([17], [18], [19], [20], [21] & [22]). In a recent work by Glushenkov et al. [3], a new concept of so-called isobaric expansion (IE) engines was described. Essentially, their approach combines the technical simplicity of the Bush thermocompressor [23] and the advantages of dense-phase working fluids, as previously adapted in few patents ([24], [25] & [26]). In [3], the authors claim that their engine could compete with the efficiency of RC/ORC-processes and could be, in contrast to numerous earlier attempts, a commercially realisable option for the utilisation of ultra-low temperature heat. The technical simplicity of such engines allows a comparably cheap realisation, making them particularly interesting for mini- and micro-scale applications [3].

As Glushenkov et al. [3] pointed out; efficient heat regeneration is the key to high thermal efficiencies of IE engines. A regenerator [27] serves to re-use heat rejected during the cooling stage of the engine cycle in a subsequent heating stage. In turn, a regenerator (and heat exchanger equipment in general) causes frictional pressure drop, while its internal volume constitutes a so-called dead volume (a compressible fluid volume not swept by the engine pistons). Both pressure drop and dead volumes tend to reduce the efficiency of piston-type heat engines ([11], [20]- [22]).

Although Glushenkov et al. [3] stated that the effects of dead volumes would be less severe than in gas-phase engines, due to the low compressibility of the dense working fluids to be used in IE engines, no quantitative evaluation of this claim was provided. Given the importance of regeneration in IE engines, more effort should be devoted to study the combined effect of regeneration efficiency and associated pressure drop as well as dead volumes on the thermal efficiency of the regenerative cycle.

Compact heat exchangers (CHE) ([28], [29]) are of special interest for this type of application because of their large surface density (> 700 m^2/m^3). This high level of compactness can either be achieved by finned surfaces or by very small dimensions of the heat exchanger channels (microchannels). Highly pressure-resistive CHE were not available when different groups, including Martini, worked on early dense-phase IE engines in the 1960s and 1970s, but they have entered the market in the recent years. Printed circuit heat exchangers (PCHE) ([30], [31] & [32]) are typical representatives of such CHE and offer new opportunities in the design of displacer-type heat engines. They are produced in a two-step procedure. First, typically semi-circular channels are chemically etched into the surface of flat plates before those plates are joined together by diffusion bonding. The result is a stack of alternating hot and cold channels, comparable to the structure of plate heat exchangers.

In this work, the thermodynamic model used by Glushenkov et al. [3] is extended to take into account the effects of internal (dead) volumes and frictional pressure drop of the required heat exchanger equipment. The individual effects of both dead volume and pressure drop on the thermal efficiency are investigated. Moreover, an approach to estimate the necessary size of such heat exchangers and the associated pressure drop is presented. Based on the results obtained with this method, a numerical study of the combined influence of regeneration efficiency, associated dead volume and pressure drop on thermal efficiency of the IE engine cycle is performed.

3.2. The thermodynamic model

A theoretical model for the thermodynamic description of isobaric expansion engines has been developed in [3] & [33]. In the present work, the model is extended on considering dead volumes and pressure drop. The model allows the engine efficiency for given temperatures of the heat source and sink to be determined. A graphical representation of the model consisting of three individual volumes, a hot volume including a heater, a cold volume including a cooler and a regenerative (heat exchanger) volume, is shown in Figure 6

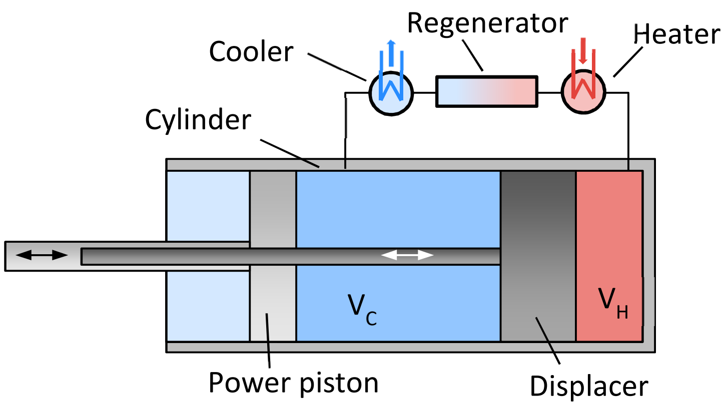

Figure 6: Thermodynamic model representing regenerative, displacer-type heat engines.

The volumes of the hot and cold domains depend on the positions of the two pistons involved: a displacer piston separating the hot and cold volume and a power piston. Any movement of the power piston results in a change in the total volume, thus performing volume work. The temperature in each individual volume is assumed to remain constant as a result of heat addition or rejection. Pressure is assumed to be equal in all domains. Frictional losses of the moving pistons are neglected. The total mass in the system expressed by Eq. (1) remains constant throughout the entire cycle:

$$m_{tot} = \rho(p, T_H)\,(V_H + V_{H0}) + \rho(p, T_C)\,(V_C + V_{C0}) + \rho(p, T_R)\,V_R \tag{1}$$

Together with an arbitrary equation of state of the form $\rho = f(p, T)$, Eq. (1) allows to calculate the instantaneous pressure for given volumes. The interdependence of the hot and cold volume defines the type of the thermodynamic cycle. In this work, the operation of the isobaric expansion engine is approximated by an ideal rectangular cycle in p-V-coordinates, consisting of two isochoric and two isobaric stages. The pressure-volume dependence for this cycle is defined by the equations listed in Table 1.

It is often useful to express the model equations shown above in terms of the swept volume of the engine, V_0. The specific work, i.e. the work produced per cycle and unit volume, is a characteristic value indicating the power density of a specific cycle. It is defined as:

$$w_{spec} = \frac{W}{V_0} = \frac{\oint p dV_{tot}}{V_0} \tag{2}$$

Table 1: Equations defining the pressure-volume-dependence of the ideal rectangular cycle.

Stage 1 → 2	$V_H = V_0 - V_C \qquad p = p_{low} \rightarrow p_{high}$ $V_C = \frac{m_{tot} - \rho(p,T_H)(V_0 + V_{H0}) - \rho(p,T_C)(V_{C0}) - \rho(p,T_R)V_R}{\rho(p,T_C) - \rho(p,T_H)}$
Stage 2 → 3	$V_H = V_{H2} \rightarrow V_0 \qquad p = p_{high}$ $V_C = \frac{m_{tot} - \rho(p,T_H)(V_H + V_{H0}) - \rho(p,T_C)V_{C0} - \rho(p,T_R)V_R}{\rho(p,T_C)}$
Stage 3 → 4	$V_H = V_{tot,3} - V_C - V_{H0} - V_{C0} - V_R \qquad p = p_{high} \rightarrow p_{low}$ $V_C = \frac{m_{tot} - \rho(p,T_C)V_{C0} - \rho(p,T_H)\left(V_{tot,3} - V_{C0} - V_R\right) - \rho(p,T_R)V_R}{\rho(p,T_C) - \rho(p,T_H)}$
Stage 4 → 1	$V_H = V_{H4} \rightarrow 0 \qquad p = p_{low}$ $V_C = \frac{m_{tot} - \rho(p,T_H)(V_H + V_{H0}) - \rho(p,T_C)V_{C0} - \rho(p,T_R)V_R}{\rho(p,T_C)}$

The required heat supply or heat rejection to/by each partial volume is determined from an individual energy balance of the respective domain i $(i = H, C, R)$, neglecting changes in kinetic and potential energies:

$$dQ_i = dU_i - dW_i - dH_i = d\left(m_i\, u(p,T_i)\right) + pdV_i - h_{i,in/out}dm_i \tag{3}$$

The last term in Eq. (3) denotes the enthalpy of fluid entering or leaving the respective domain. If working fluid enters the domain i, i.e. $dm_i > 0$, $h_{i,in/out}$ equals the enthalpy at the interface of domain i and the adjacent domain from which the fluid enters. Working fluid leaving the domain i, i.e. when $dm_i < 0$, has the same enthalpy as the bulk fluid in this domain ($h_{i,in/out} = h_i$).

The efficiency of the cycle is defined as the ratio of useful work produced to the amount of heat supplied during a full cycle:

$$\eta = \frac{w_{spec}V_0}{Q_H} = \frac{\sum_i \oint dQ_i}{\oint dQ_H} = \frac{\sum_i \oint pdV_i}{\oint dQ_H} \tag{4}$$

The term Q_H in Eq. (4) represents the overall heat added to the engine, which can be determined by integrating Eq. (3) for the hot part (i = H). The difference in enthalpy streams leaving and entering the hot volume largely influences the required heat supply Q_H. The temperature of working fluid leaving the hot space is known (TH), and h_{out} can be calculated directly. The temperature of working fluid flowing into the hot space (coming from the regenerator) is, however, unknown and depends on the quality of the regenerative process. The regenerator serves to re-use heat rejected during the cooling period, to preheat the cold working fluid during a subsequent heating period. If no regenerator were present, the inflow temperature would be TC. If regeneration takes place, the inflow temperature will be somewhat elevated, depending on the performance of the regenerator. In the case of ideal working fluids, perfect regeneration (T_{in} = TH) is theoretically possible, whereas in the case of non-ideal working fluids, thermodynamic limitations require that the net enthalpy flow out of the hot space per cycle cannot be zero [34] even if T_{in} = TH. Estimating the maximum possible regeneration is an important step towards prediction of the potential efficiency of regenerative heat engines with non-ideal working fluids.

3.3. Regeneration efficiency

As previously described, the regenerator is a core element of IE engines. If effective regeneration is realised, the required heat supply to drive the engine can be minimised. As indicated in the previous section, perfect regeneration is not possible because of thermodynamic limitations. Which is the main reason for imperfect regeneration results from different heat capacities in the heating phase (at high pressure) and during the cooling (at low pressure) in the regenerator. In the literature, the effectiveness of a heat exchanger is usually defined as the ratio of the actual enthalpy change of the fluid passing through the apparatus to the maximum (thermodynamically allowed) enthalpy change ([35]):

$$\varepsilon_R = \frac{Q_{R,act}}{Q_{R,max}} \tag{5}$$

The smaller the driving temperature difference of the heat exchange process, the closer the effectiveness approaches the value 1. In the case of ideal gases, perfect regeneration is theoretically possible, since enthalpy does not depend on pressure and is a function of temperature only. Hence, Eq. (5) is enough to describe the performance of the regeneration process.

If non-ideal working fluids are applied, the situation is different, with enthalpy depending on both temperature and pressure. As perfect regeneration is not possible in such a case, it is necessary to determine the maximum amount of heat to be transferred in a regeneration process. We estimate this maximum enthalpy change during the regeneration process by comparing the cumulative enthalpy functions of the heat-receiving fluid and the heat-delivering fluid. These functions are defined under assumptions that:

- the heat capacity of the regenerator is much larger than that of the working fluid (i.e., the regenerator temperature does not change during the cycle)
- heat transfer along the length of the regenerator is negligible
- the residence time of the working fluid in the regenerator is much lower than the cycle period

The cumulative enthalpy functions are defined as:

$$H_{Rec}(T) = \int_{m_{min}}^{m_{max}} h(T,p)dm \tag{6}$$

and

$$H_{Del}(T) = \int_{m_{max}}^{m_{min}} h(T,p)dm \tag{7}$$

with subscripts [Rec] and [Del] denoting the heat-receiving phase at higher pressure and the heat-delivering phase at lower pressure in the regenerator, respectively. An example of these functions is illustrated in Figure 7a.

Heat is transferred from the hot (delivering) fluid (via thermal storage in the regenerator) to the cold (receiving) fluid through the regenerator body. This process is possible if the temperature of the regenerator exceeds the temperature of the receiving fluid throughout the regenerator. This is realised by shifting the high-pressure enthalpy curve far enough along the enthalpy axis:

$$H_{Rec,shift}(T) = \int_{m_{min}}^{m_{max}} h(T,p)dm + \Delta H_{shift} \tag{8}$$

The least necessary shift $\Delta H_{shift,min}$ can be estimated when both curves first touch each other at one point without crossing (Figure 7b). The enthalpy change during regeneration can then be calculated as:

$$\Delta H_{R,max} = H_{Del}(T_H) - H_{Rec,shift,min}(T_C) \tag{9}$$

In case of ideal gases as working fluids, i.e. identical cumulative enthalpy curves for heating and cooling, perfect regeneration is theoretically possible (Figure 7d). For non-ideal working fluids, it is useful to relate the maximum enthalpy change by regeneration to the required total enthalpy change from T_C to T_H:

$$\eta_{R,max} = \frac{\Delta H_{R,max}}{H_{Rec}(T_H) - H_{Rec}(T_C)} \tag{10}$$

In a real regenerator, heat transfer is driven by a positive, non-zero temperature difference at each point. This requires an additional shift of the high-pressure enthalpy curve and reduces the possible enthalpy change in the regenerator (Figure 7c). To describe the regenerator performance in processes involving non-ideal working fluids, one has to take into account both the thermodynamic limitations of regenerative heat transfer, i.e. the maximum value defined by Eq. (10), and the regenerator effectiveness (cf. Eq. (5)) as a function of the actually realized minimum temperature difference. This is necessary, because the maximum regeneration ratio $\eta_{R,max}$ can be different for different working fluids, cycles and operating conditions. It is thus reasonable to define the product of both quantities as actual regeneration efficiency:

$$\eta_R = \frac{\Delta H_R}{H_{Rec}(T_H) - H_{Rec}(T_C)} = \varepsilon_R \cdot \eta_{R,max} \tag{11}$$

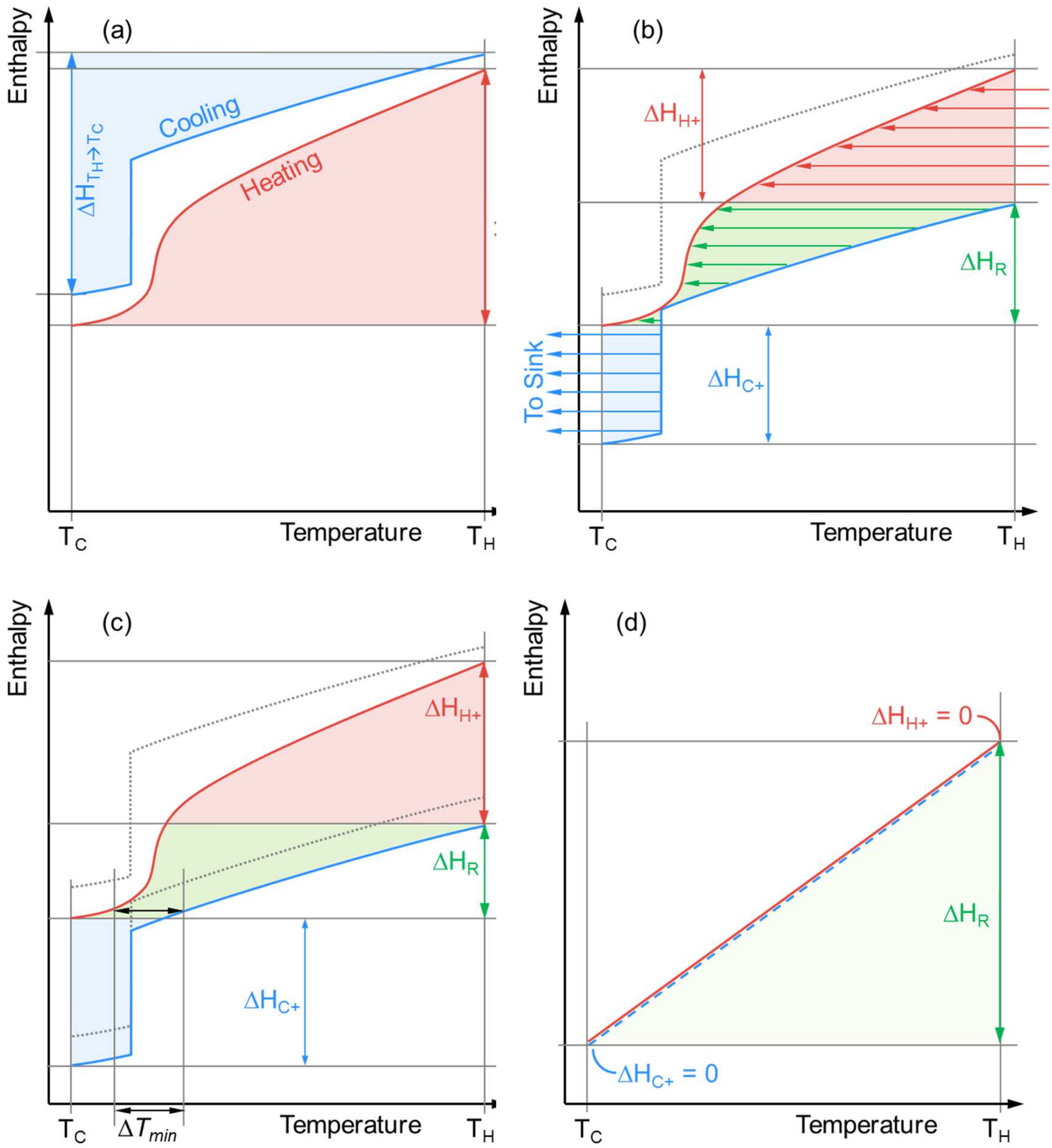

Figure 7: Example of cumulative enthalpy curves for heating and cooling; (a) original positions, (b) cooling curve shifted, so that ΔTmin = 0, (c) cooling curve shifted further to obtain a certain ΔTmin, (d) cumulative enthalpy curves for an ideal gas and ΔTmin = 0.

3.4. Heat exchanger design

At first glance, regeneration of heat improves the efficiency of the thermodynamic cycle. In real engines, however, regeneration and heat transfer in general take place in heat exchangers, generating pressure loss and dead volumes (internal volumes). This in turn, tends to reduce efficiency. In an approach to capture the interdependence of regeneration, dead volumes, pressure drop and their combined effect on the cycle efficiency, we developed a simplified design method for the required heat exchangers. Dimensions are determined based on the following assumptions:

- Only the isobaric stages are taken into account for the heat exchanger design; heating/cooling takes place at constant high/low pressure, respectively.

- The residence time of the working fluid in the heat exchangers is small compared to the duration of a half cycle (i.e., heating or cooling period). Hence, quasi-steady-state flow and heat exchange is assumed.
- Heat is recovered in a recuperative heat exchanger, which could be realised by a duplex arrangement of two IE engines operating in counter-phase [3]. Effectively, this eliminates the thermal storage of a regenerator matrix, and heat is transferred directly from the heat-delivering fluid to the heat-receiving fluid.
- Additional heating and cooling, i.e. heat transfer required to compensate non-ideal regeneration, is performed in heat exchangers with a fixed mean temperature difference. Heat transfer resistances on the heat carrier or cooling agent side of these heat exchangers are neglected.

Table 2: Estimated heat duties for steps 1 (recuperation) and 2 (additional heating and cooling to hot/cold space temperature).

Recuperative heating (step 1)	$\dot{Q}_{R,H} = \dot{M}_{av}\left[h_{R,H} - h\left(T_C, p_{high}\right)\right]$
Heating to T_H (step 2)	$\dot{Q}_{\to T_H} = \dot{M}_{av}\left[h\left(T_H, p_{high}\right) - h_{R,H}\right]$
Recuperative cooling (step 1)	$\dot{Q}_{R,C} = -\dot{Q}_{R,H} = \dot{M}_{av}\left[h_{R,C} - h(T_H, p_{low})\right]$
Cooling to T_C (step 2)	$\dot{Q}_{\to T_C} = \dot{M}_{av}\left[h(T_C, p_{low}) - h_{R,C}\right]$

Estimation of the heat duties of the heater, cooler and regenerator is necessary to determine their size, internal volume and pressure drop. These values are estimated by applying the cumulative enthalpy approach described in the previous section for the isobaric cooling and heating (cf. Figure 8). In this case, the cumulative enthalpy function for the high-pressure fluid becomes:

$$\dot{H}_{Rec}(T) = \dot{M}_{av}\, h\left(T, p_{high}\right) \tag{12}$$

with

$$\dot{M}_{av} = 2\, f\, \rho\left(T_H, p_{high}\right) V_0 \tag{13}$$

The procedure for the low-pressure fluid is similar. After estimating the regenerator outlet enthalpies $h_{R,H}$ and $h_{R,C}$, the heat duties of heater, cooler and regenerator can be determined using the equations listed in Table 2.

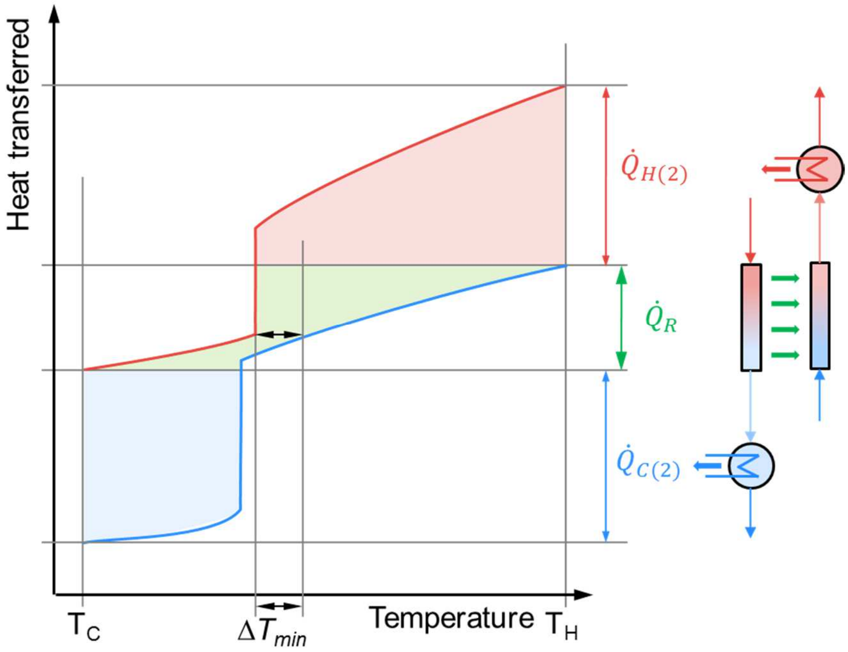

Figure 8: Cumulative enthalpy curves to determine heat duties for heater, cooler and recuperator for a given minimum temperature difference (left) and sketch of the involved heat transfer processes (right).

To determine the required heat exchanger surfaces, each individual heat exchanger is subdivided into several segments in each of which an equal amount of heat is transferred. The surface area of a segment x is calculated from:

$$\dot{Q}_x = k_x \, A_x \, \Delta T_{m,x} \tag{14}$$

The overall heat transfer coefficient k_x per segment is calculated using appropriate heat transfer correlations depending on local fluid properties and flow parameters. The mean temperature difference $\Delta T_{m,x}$ per segment is found from the cumulative enthalpy functions (for recuperative heat transfer, step (1)) or is given as a fixed value for additional heating and cooling steps (step 2).

The heat exchangers are modelled as arrays of parallel straight tubes. The required number of tubes and their length is determined as a function of the required heat transfer surface for specified internal tube diameters and flow velocity restrictions. The pressure drop along these tubes is determined from:

$$\Delta p_{fr,x} = \xi_x \, \frac{L_x}{d_{h,x}} \, \frac{\rho_x \, w_x^2}{2} \tag{15}$$

Appropriate correlations are used to evaluate the local friction factor ξ_x.

The full list of heat transfer and pressure drop correlations used in this work is given in Table 3. The correlations were carefully selected for the individual flow regimes and geometric dimensions and are widely accepted methods.

Table 3: Flow- and geometry-specific heat transfer and pressure drop correlations used in this paper.

	Heat transfer		Pressure drop	
	Macro-scale	*Micro-scale*	*Macro-scale*	*Micro-scale*
Single-phase flow	Gnielinski [36]		Konakov [37]	
Boiling	Steiner&Taborek [38]	Thome et al. [39]	Mueller-Steinhagen&Heck [40]	
Condensation	Numrich&Müller [41]	Cavallini et al. [42]	Numrich&Müller [41]	Cavallini et al. [42]
Transcritical flow	Gnielinski [36]		Konakov [37]	

Calculation procedure

Figure 9 shows how the models described above are coupled in order to determine the efficiency of a regenerative IE engine with due consideration of the negative effects of dead volumes and pressure drop, arising because of heat regeneration.

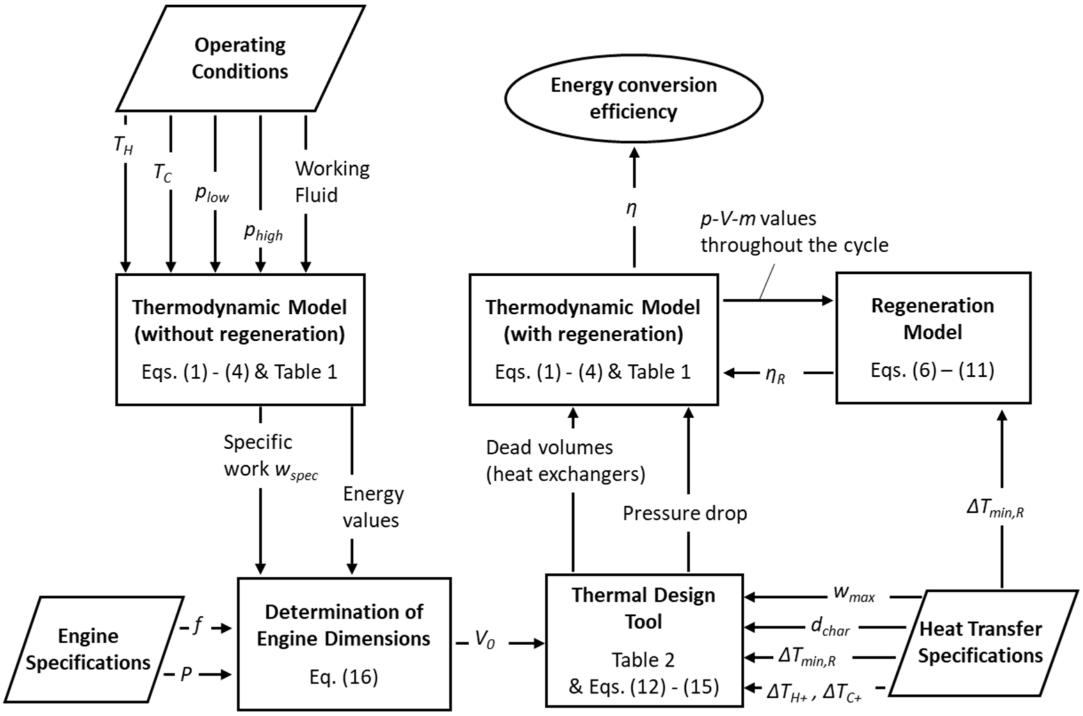

Figure 9: Scheme of the calculation procedure for the determination of the combined effect of regeneration, dead volumes and pressure drop on the energy conversion efficiency.

In a first step, the performance of the non-regenerative cycle without dead volumes and pressure drop is determined for predefined operating conditions. The variable of interest is the specific work performed per cycle under these conditions. It is necessary to determine the required size of the engine, characterised by the swept volume V_0, to generate the desired power output P at a defined operation frequency f:

$$V_0 = \frac{P}{w_{spec} f} \tag{16}$$

The next step is the thermal design of required heat exchangers, heater, cooler and regenerator. The lengths, internal volumes and affiliated frictional pressure losses are determined for certain heat transfer specifications, mainly the desired degree of regeneration (expressed by the minimum temperature difference during regeneration).

The results of the thermal design are used as input values for another thermodynamic simulation, now considering dead volumes and pressure drop as well as regeneration. In this process, the thermodynamic simulation interacts with the regeneration model in order to determine the regeneration efficiency for the specified $\Delta T_{min,R}$. This ultimately results in the energy conversion efficiency of the regenerative heat engine.

Printed circuit heat exchangers for IE engines

The heat exchangers of isobaric expansion engines need to be designed compactly in order to minimise dead volumes detrimental for the engine efficiency. So-called printed circuit heat exchangers (PCHE) ([30]- [32]) are an interesting option for this application. They are produced by chemically etching small-diameter channels, typically of semi-circular shape, into thin plates. These plates are then stacked in an alternating order for hot and cold fluid and joint together by diffusion bonding. The result is a very compact and highly pressure and temperature resistant heat exchanger, as depicted in Figure 10. An advantage of PCHE is design flexibility and the possibility to manufacture channels with very small diameters [43].

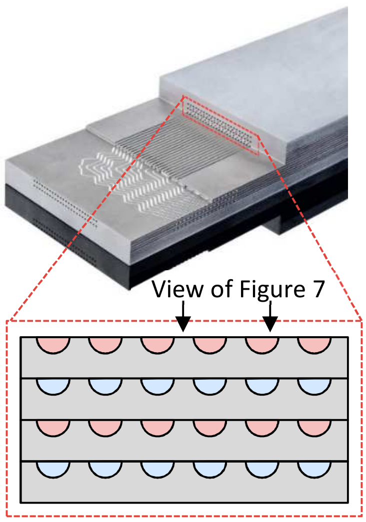

Figure 10: Printed circuit heat exchanger (above, courtesy of Vacuum Process Engineering) **[44]** *and schematic illustration of the channel arrangement (below).*

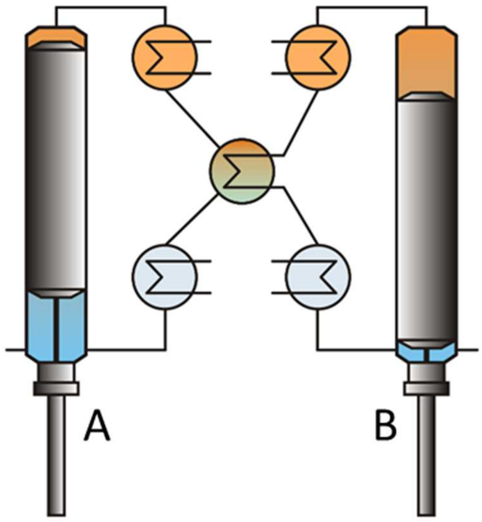

Figure 11: Duplex arrangement of two individual IE engine units (A and B) coupled by a common recuperative heat exchanger **[3]**.

Glushenkov et al. [3] presented a possible design of IE engines in a so-called duplex arrangement (Figure 11). Two separate engine units operating in counter-phase share a common heat exchanger block. This enables the re-use of rejected heat in a recuperative process to be realised instead of cyclically accumulating and releasing heat in a thermal storage (e.g., a matrix of solid material). However, each engine unit needs its own set of channels for cooling and heating.

A possible design of such a heat exchanger unit is depicted in Figure 12. It consists of an alternating arrangement of plates of four different types: (1) Cooling plates for working fluid from engine A, (2) heating plates for working fluids from engine A, (3) cooling plates for working fluid from engine B and (4) heating plates for working fluid from engine B. In the stacked arrangement, working fluid enters the plates either at the top (cooling plate) or bottom (heating plate) of the recuperative zone and is distributed into the multiple working fluid channels (straight lines with colour gradient in Figure 12; each straight line corresponds to a single channel shown in Figure 5). Hot (heat-delivering) working fluid, flowing through the channels of a cooling plate, rejects heat to initially cold (heat-receiving) working fluid, flowing in an adjacent heating plate in the recuperative zone. Since the recuperative heat transfer is generally insufficient (see Section 3.3), additional cooling of the heat-delivering stream and additional heating of the heat-receiving stream are necessary. Additional heating is realised by a heat carrier, flowing through respective channels in the top section of a cooling plate and supplying heat to the heat-receiving fluid in an adjacent (heating) plate. Analogously, a cooling agent flowing in the bottom section of a heating plate withdraws heat from the working fluid in an adjacent cooling plate. By this means, the heat exchanger scheme depicted in Figure 11 can be realised in a single block.

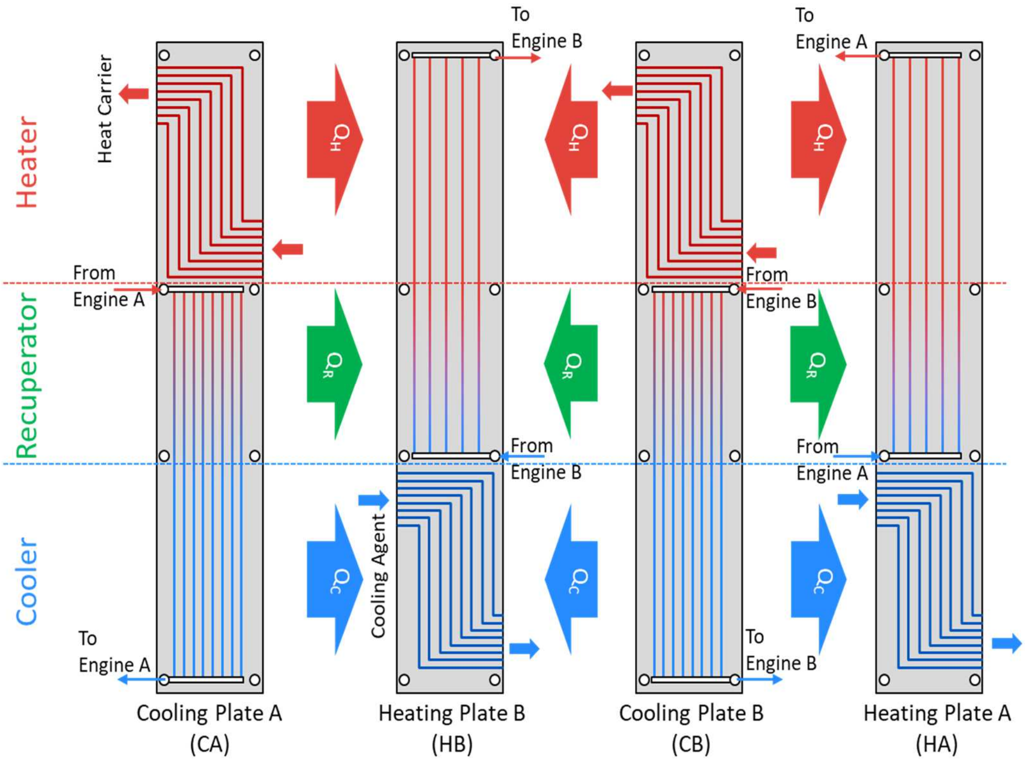

Figure 12: Possible arrangement of alternating PCHE-plates in a heat exchanger for IE engines. Cooling plates and heating plates are stacked in an alternating and repeating order (CA-HB-CB-HA-CA-HB-…). Heat is transferred from heat-delivering working fluid to heat-receiving working fluid in the recuperative (middle) section, from heat-delivering working fluid to a cooling agent in the cooling (bottom) section or from a heat carrier to heat-receiving working fluid in the heating (upper) section.

The application of PCHE allows an individual channel design for each plate. By this means, the number of channels in cooling plates could be different to that in heating plates in order to avoid very high or low fluid flow velocities.

3.5. Results and discussion

Influence of dead volume and pressure drop

Previously, it has been shown that recuperation/regeneration can potentially lead to a significant efficiency improvement in heat engines of the investigated type ([3], [33]). In these studies, however, the influence of internal volumes on heat exchanger equipment (i.e., dead volumes [11] and frictional losses (pressure drop)) were neglected. Calculations using the extended model enable these aspects to be studied in more detail. The negative influence of pressure drop (see Figure 13) can easily be explained by the fact that a fraction of the produced work is spent to overcome flow resistances:

$$\eta = \frac{W - \Delta p_{fr} V_0}{Q_H} = \eta_0 \left(1 - \frac{\Delta p_{fr}}{w_{spec}}\right) \tag{17}$$

The effect of dead volumes is more intricate. It results from the displacement of the working fluid from the cold space to areas not swept by the piston or displacer in order to compensate fluid compressibility during the first (isochoric) stage of the rectangular cycle. Accordingly, a smaller fraction of the swept volume V0 (total displacement) is available to be displaced during the second stage of the cycle, in which useful work is produced.

As Figure 14 illustrates, the severity of this effect depends on the compressibility of the working fluid at a constant temperature. While nearly incompressible fluid volumes (typical for the fluid in the cold space) show only a reduced influence on the efficiency, dead volumes in which the working fluid is in gaseous state, and therefore highly compressible, causing significant efficiency drop. Consequently, designing heat exchangers and recuperators for isobaric expansion engines is a difficult task, as the positive effects of recuperation may be reduced by the dead volume effect of required heat exchanger equipment and frictional pressure drop. A decision, as to which degree of recuperation is reasonable, with due account of these effects, requires performing calculations with full consideration of the combined influence of efficiency improvement through recuperation, necessary dead volumes and pressure drop. This issue is discussed in the subsequent Section.

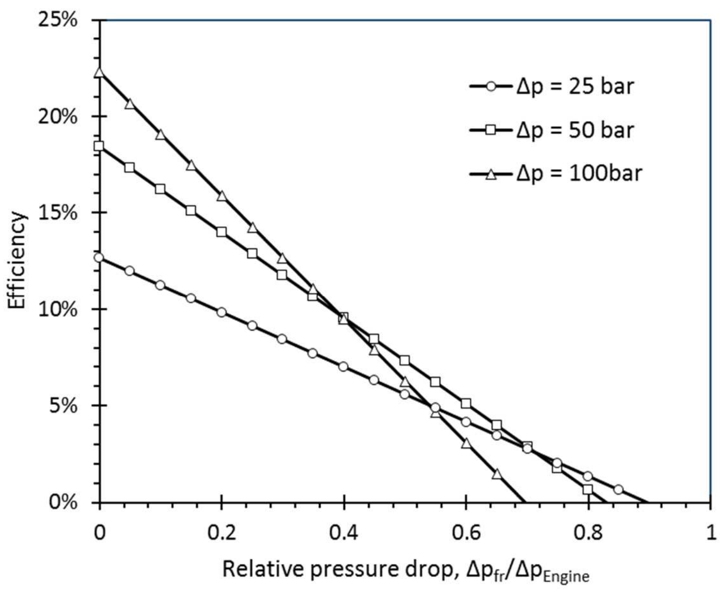

Figure 13: Influence of pressure drop (Δpfr) on thermal efficiency for R32 (TC = 40 °C, TH = 200 °C), recuperation with ΔTmin = 5 K for pressure differences (ΔpEngine = phigh - plow) of 25, 50 and 100 bar.

Combined effect of recuperation, pressure drop and dead volume

To reach high recuperation efficiencies, one needs to decrease the minimum temperature difference in the recuperation process (cf. Figure 7 and Figure 8). All other things being equal, this would lead to an increase in the required heat transfer surface, according to Eq. (14), i.e., larger heat exchangers with higher dead volume. A way to decrease dead volumes is to apply very compact heat exchangers with large surface-to-internal volume ratios. Compact heat exchangers with very narrow channels, such as PCHE (cf. Section 3.4) are one option. A second possibility is to increase the flow velocity of working fluid, leading to intensified heat transfer at higher Reynolds numbers. Both options, cause elevated pressure drop, also having a negative effect on the efficiency, potentially voiding the intended benefits of recuperation.

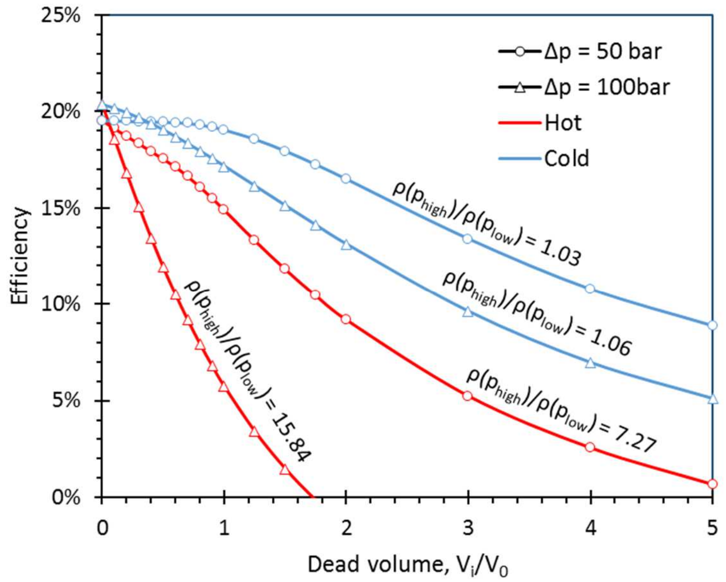

Figure 14: Influence of hot and cold dead volumes on thermal efficiency for R134a (TC = 40 °C, TH = 200 °C), recuperation with ΔTmin = 5 K for pressure differences of 50 and 100 bar.

Hence, it is necessary to explore the impact of heat exchanger design decisions, with their specific pressure drop and dead volume, on the efficiency of a recuperative IE engine. For this purpose, a numerical study, following the algorithm explained in Section 3.4, is performed.

In the first case study, propane was selected as working fluid, with temperatures of the hot and cold space equal to 200 °C and 40 °C, respectively. An engine pressure difference of 100 bar is chosen. A displaced volume of each engine in the duplex arrangement (cf. Figure 11) of 0.738 L and an operation frequency of 0.125 Hz were chosen. Under these conditions, the resulting power output (cf. Eq. (6)) is approximately 1 kW, determined with the specific work obtained from Eq. (2). For a maximum flow velocity of 10 m/s, several characteristic diameters of the heat exchanger channel size, ranging from 0.5 to 5 mm, were investigated.

The results are displayed in Figure 15. The general trend shows increasing efficiency with increasing recuperation efficiency (i.e. decreasing minimum temperature difference in the regenerator). Without recuperation, the thermal efficiency is as low as 3.2% (for d = 0.5 mm) and can be increased up to 18.2% (at ΔTmin = 3 K, 54% of Carnot efficiency). When approaching ideal recuperation, however, the efficiency begins to drop. This can be explained by the disproportionate increase of the required heat transfer area (i.e., heat exchanger length) and pressure drop necessary to achieve very low temperature differences in the regenerator (see Figure 16). Moreover, the results clearly display that the efficiency is closest to ideal efficiency (i.e. efficiency without pressure drop and dead volume) for small characteristic sizes of the heat exchanger channels. Hence, it can be concluded that the compactness of mini-sized heat exchanger channels, resulting in smaller dead volumes, outweighs the elevated pressure drop of these narrow channels.

Another aspect to be considered is the relationship of the heat exchanger length and average flow velocity, i.e., the residence time in the heat exchanger. If residence times are high compared to the duration of the heating or cooling periods (half cycle time), incomplete heating or cooling occurs. Consequently, the fluid will enter the hot (cold) space with a lower (higher) temperature than intended during a significant part of the heating (cooling) period. As the negative influence of this effect cannot be quantified in our isothermal approach, a maximum ratio of residence time to half cycle time of 20% is applied. Below this threshold, no significant negative influence on the efficiency is expected. In Figure 15, thick lines with markers indicate this restriction being complied, whereas thin lines are shown wherever the 20% threshold is violated.

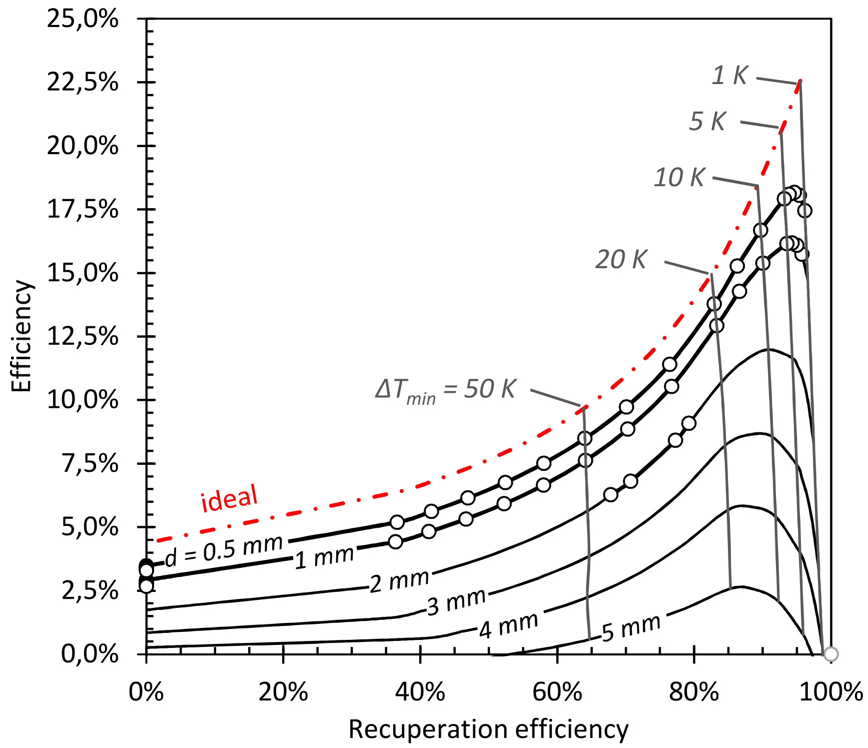

Figure 15: Effect of recuperation on the efficiency for propane (TC = 40 °C, TH = 200 °C, ΔpEngine = 100 bar) with different characteristic sizes of heat exchanger channels (d = 0.5 – 5 mm) at a maximum flow velocity of 10 m/s. Thick curves with markers correspond to residence times lower than 20% of the half cycle time, thin lines without markers correspond to the opposite cases.

Figure 15, shows that this restriction is particularly serious for heat exchangers with relatively large channel sizes (d > 1 mm) and when highly efficient recuperation is desired. For instance, at d = 2 mm, this restriction allows operation only within a narrow range of recuperation efficiencies between 67.8 and 79.2% (relating to ΔTmin = 27.1 – 44.6 K). A temperature difference smaller than 27.1 K would require a too long recuperative unit of the heat exchanger, whereas a temperature difference above 44.6 K would result in an excessively long heater unit, both resulting in significantly large transit times. At characteristic diameters below 1 mm, the heat exchangers are sufficiently compact to ensure that the required length of the heat exchanger units is low enough to comply with the residence time restriction. Hence, such mini-sized heat exchangers are of great interest for application as IE engine heat exchangers, because their compactness allows to realise highly efficient recuperation and, consequently, high thermal efficiency.

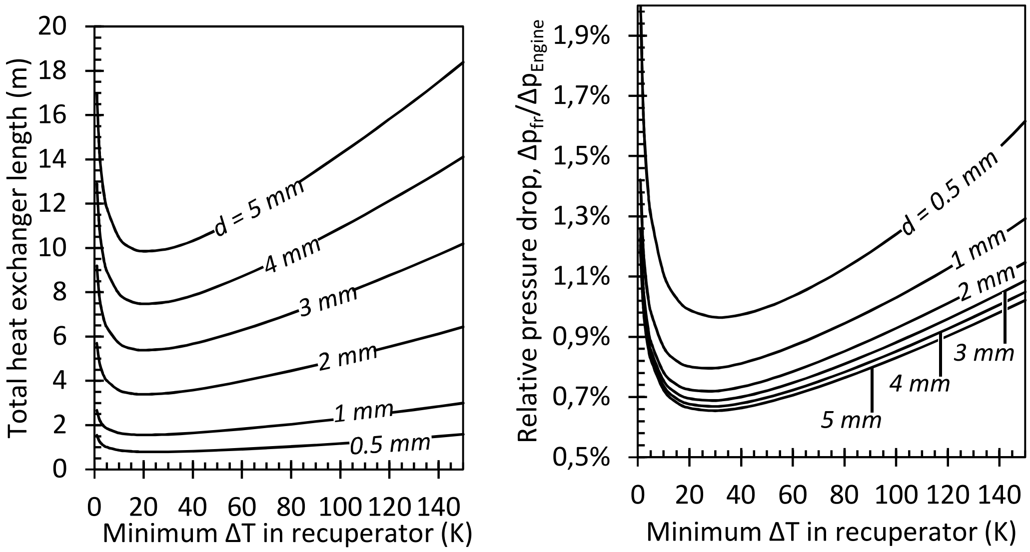

Figure 16: Required length of (left) and resulting pressure drop in (right) the heat exchanger unit (heater, regenerator and cooler) for propane (TC = 40 °C, TH = 200 °C, ΔpEngine = 100 bar) in dependence on minimum temperature difference during recuperation for different characteristic sizes of heat exchanger channels (d = 0.5 – 5 mm) at a maximum flow velocity of 10 m/s.

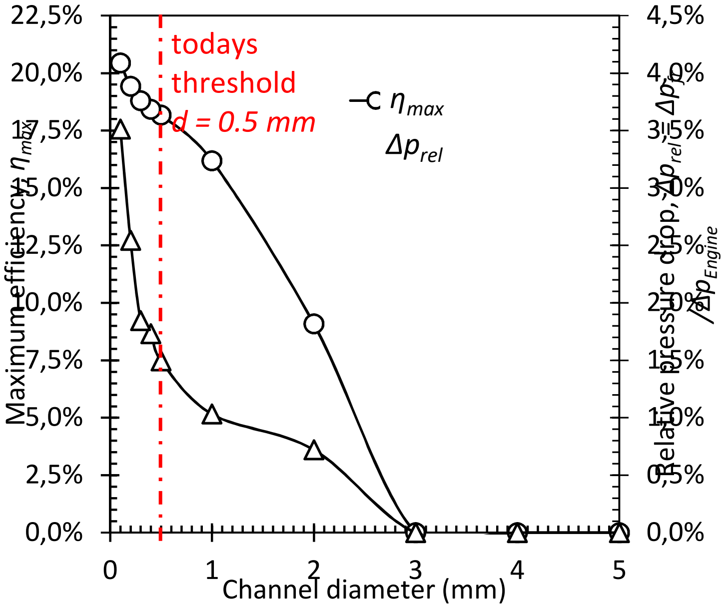

Figure 17: Maximum efficiency of the recuperative cycle and relative pressure drop for different channel sizes for propane (TC = 40 °C, TH = 200 °C, ΔpEngine = 100 bar) at a maximum flow velocity of 10 m/s, including an outlook on the effect of very narrow channels (dch < 0.5 mm).

For the major part of this study, a minimum channel diameter of 0.5 mm was chosen, which is often cited as the smallest feasible diameter from a manufacturing perspective [30]. As manufacturing technologies and materials evolve, smaller dimensions may be feasible in the future. Figure 17 shows how the maximum efficiency in our example could be improved by further reducing the diameter. Notably, the pressure drop rapidly increases at such small diameters and may become critical.

Effect of recuperation for different grades of heat sources

In a comprehensive simulation study, heat sources of different grade (T_H = *80 °C*, *120 °C* and *200 °C*) were considered and the effect of recuperation on the thermal efficiency of the cycle was investigated. Here, we discuss only the combinations of working fluid and engine pressure difference that were found to be the most promising applications for each heat source temperature. These cases are listed in Table 4.

Table 4: Detailed characteristics of the combinations of working fluids, hot-space temperatures and pressure differences presented in Section 3.

	Case I	*Case II*	*Case III*	*Case IV*
Working fluid	R32	R32	R32	Pentane
Hot space temperature, T_H (°C)	200	120	80	80
Cold space temperature, T_C (°C)	40	40	40	40
Engine pressure change, Δp_{Engine} (bar)	100	50	25	2
Maximum flow velocity, w_{max} (m/s)	15	10	10	10
Cycle frequency, f (Hz)	0.125	0.125	0.125	0.125
Swept volume per engine, V_0 (L)	0.575	1.072	1.994	20.3
Power output of duplex unit, P (W)	1000	1000	1000	1000

The results shown in Figure 18 display that the importance of effective recuperation increases with rising temperature of the heat source.

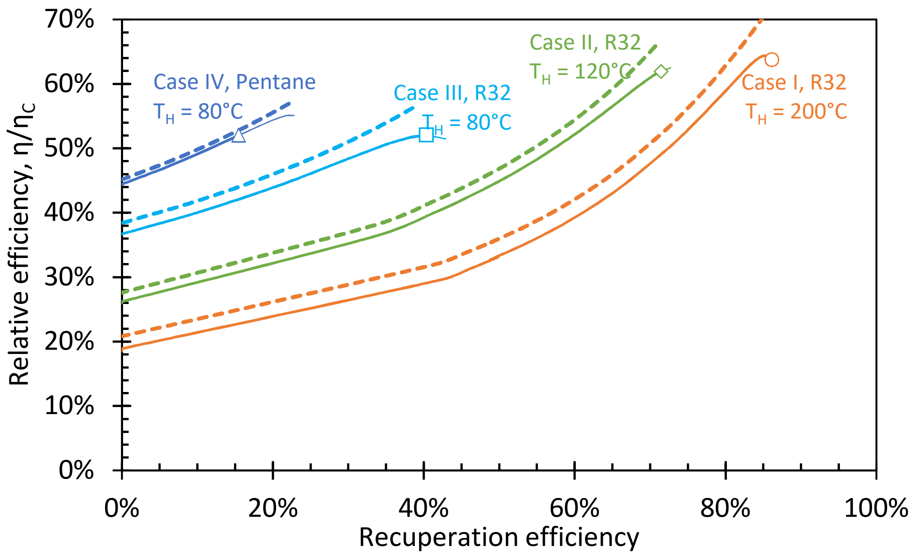

Figure 18: Relative efficiencies in dependence on recuperation efficiency for the cases listed in Table 4. Dashed lines indicate the ideal efficiency (neglecting dead volumes and pressure drop), markers indicate the maximum recuperation efficiency in agreement with the residence time restriction (tRes > 0.2 tcy/2). The heat exchanger channel size was chosen as d = 0.5 mm for each case.

Without recuperation, the efficiency of the process at T_H = *200 °C* is as low as 6% (< 20% of Carnot efficiency) but can be increased up to nearly 65% of Carnot efficiency using highly efficient small-scale recuperative heat exchangers. At very low heat source temperatures (T_H = *80 °C*), the positive effect of recuperation is less pronounced. For R32 and Δp_{Engine} = *25 bar*, the relative efficiency could be improved from 37% to 52%. At such low temperatures, it is questionable, whether this rather small increase in efficiency justifies the expenses of highly efficient heat transfer equipment. The relative efficiency in another ultra-low temperature case (pentane at Δp_{Engine} = *2 bar*) was found to be already at 45% (without recuperation), which makes this case an interesting option for a very simple, non-regenerative design of IE engines.

3.6. Selection of working fluids

Preliminary considerations

The properties of an ideal working fluid for an IE engine operated on a rectangular cycle can be deducted from the governing equations. A suitable working fluid should offer both high specific power (work per cycle and engine volume) and efficiency. The specific power in the ideal case of zero dead volumes can be derived from the equations listed in Table 1.

$$\frac{W}{(p_h - p_l)\, V_0} = \Delta V_{tot} = \left(\frac{\rho(p_l, T_C)}{\rho(p_h, T_C)} - \frac{\rho(p_h, T_H)}{\rho(p_h, T_C)} \right) = \kappa - \epsilon^{-1} \tag{18}$$

The specific work is maximised, if the fluid is incompressible in its cold state ($\kappa = 1$) and has maximum thermal expansion ($\epsilon \to \infty$) at the high cycle pressure. A few values of κ and ϵ are listed in Table 5, clearly pronouncing the benefits of dense working fluids over gaseous working fluids. Larger specific power facilitates smaller machines and/or decreasing the operation frequency significantly. High-frequency operation is responsible for some of the most severe difficulties in state-of-the-art displacer-type heat engines with gaseous working fluids. Despite having a poor power density, gaseous working fluids theoretically allow for perfect regeneration [45]. In contrast, the regeneration potential of dense working fluids is limited.

Table 5: Values of compressibility κ and thermal expansion ϵ for selected working fluids for TC = 40°C and TH = 150°C.

	Operating pressure p_{low} | p_{high} (bar)	Compressibility κ (-)	Thermal expansion ϵ (-)
Helium	1.0 | 1.2	1.1999	1.351
Water	1.0 | 3.0	1.0001	629.134
n-Pentane	1.2 | 3.0	1.0004	94.052
R32	25.2 | 50.0	1.0286	10.178

The difficulty in finding an optimal working fluid for IE engines is to identify fluids with both large specific power and similar courses of the cumulative enthalpy curves. In the subsequent sections of this paper, we analyse the performance of several interesting working fluids. These fluids listed in Table 6 were selected for further investigation after performing a preliminary study of a large variety of working fluids. The thermodynamic model explained in the previous section has been implemented in MATLAB and is numerically solved in order to determine each fluids performance. Required fluid properties are calculated using REFPROP 9.1 [46]. For the efficiency calculations in the subsequent sections, best possible regeneration, i.e. a pinch temperature *(ΔT_{min})* of *0 K* is assumed.

Table 6: Promising working fluids selected for further investigation within this paper and their critical data.

	Saturation pressure at $T_C = 40°C$ (bar)	Critical pressure p_{crit} (bar)	Critical temperature T_{crit} (°C)
Difluoromethane (R32)	25.02	57.95	78.20
Isobutane (R600a)	5.37	36.29	134.66
Isopentane (R601a)	1.53	33.78	187.20
Propane (R290)	13.83	42.51	96.74
Propane/Pentane *(35-65 wt.-%)*	8.79	45.29	157.19

Dense working fluids with phase change

In contrast to gaseous working fluids, on which most displacer-type heat engines are operated, dense working fluids with phase change are liquid at the low cycle temperature and are evaporated when displaced to the hot volume of the engine. The liquid cold fluid is easier to seal and can serve as a lubricant for rubbing parts (e.g. the driving mechanism of the displacer) and tolerates more dead volume due to its low compressibility. Moreover, the high thermal expansion during liquid-vapour transition allows to generate large pressure changes during a cycle and significantly larger specific power (work per cycle and unit engine volume), consequently.

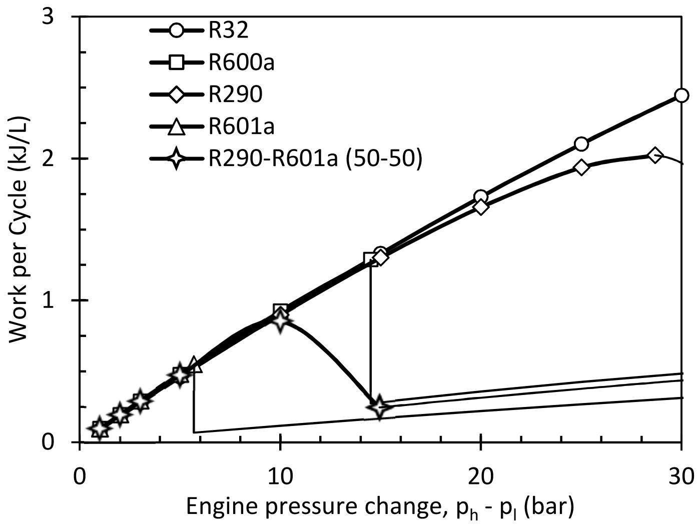

Figure 19: Simulated specific work per cycle for different working fluids in dependence on the pressure change during the cycle, TC = 40°C, TH = 100°C.

The achievable work per cycle and efficiencies for a number of such fluids is indicated in Figure 19 and Figure 20 for different hot space temperatures and pressure changes generated by the engine. These energy conversion efficiencies are calculated based on the assumption of best possible regeneration (see previous section). For all studied cases, the cold space temperature T_C was fixed at 40°C. The low cycle pressure p_{low} should barely exceed the saturation pressure at T_C in order to prevent boiling in the cold space at any moment. For the fluids investigated, the maximum pressure change *($\Delta p = p_{high} - p_{low}$)* is around 30 bar before p_{high} exceeds the critical pressure or the saturation pressure at T_H. The latter would result in undesired condensation of hot working fluid and strongly deteriorate the engines efficiency. The results shown in Figure 20 indicate that the highest efficiencies are usually obtained when the pressure change in the engine is large. At hot temperatures of T_H = *150*, *200* and *300°C*, efficiencies of up to 57.5%, 54%

and 51% of Carnot efficiency, respectively, are found using propane as working fluid. Notably, in comparison to the other working fluids, propane has both a low critical temperature and a relatively low critical pressure.

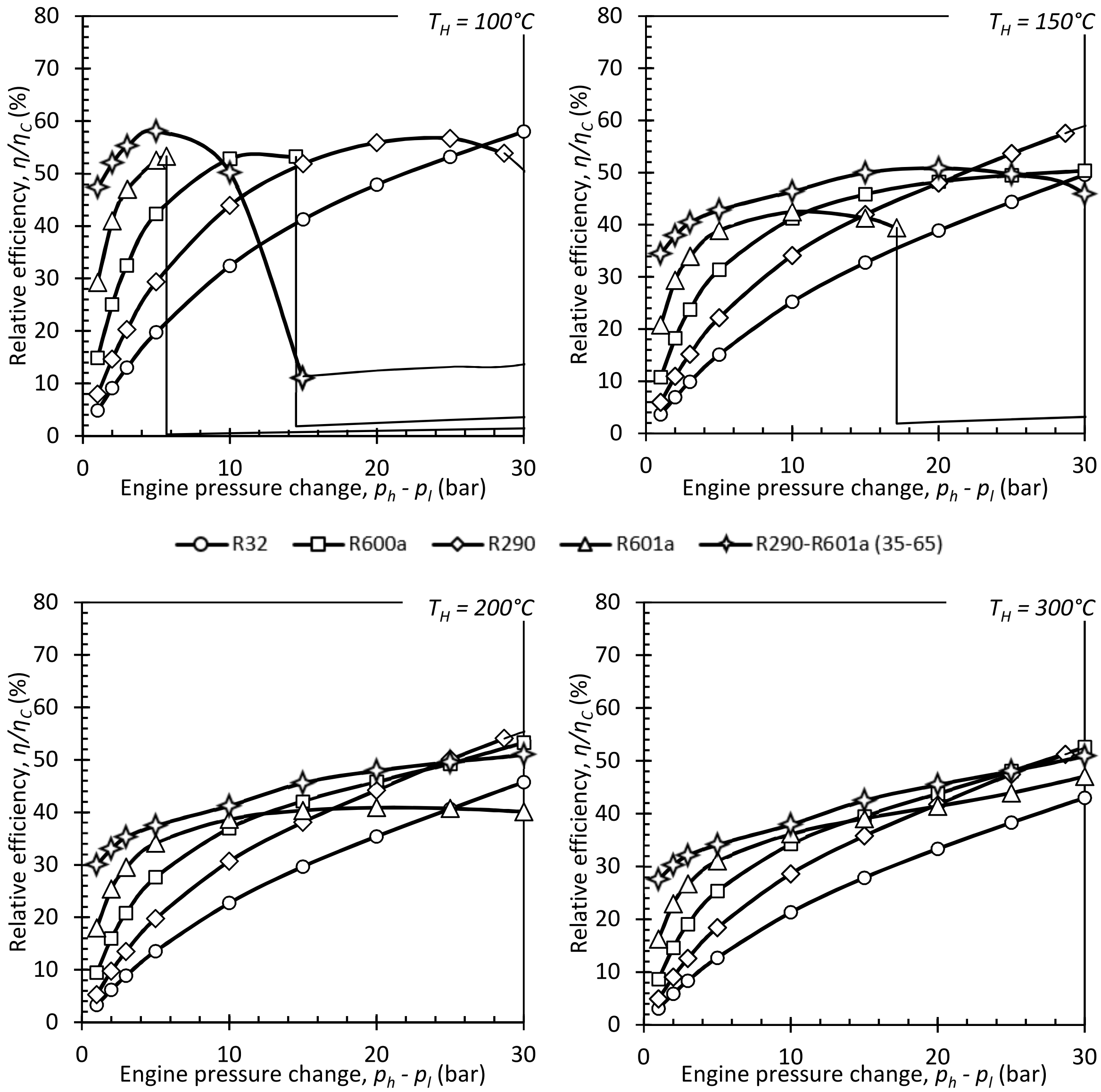

Figure 20: Simulated maximum energy conversion efficiencies at TC = 40°C and different values of TH for several subcritical working fluids in dependence on the engine pressure change and in relation to the respective Carnot efficiency.

Analysing the results at T_H = *100°C* it cannot only be found that R32 promises the largest efficiency (58% of η_C at *Δp = 30 bar*). Moreover, very high efficiencies can also be found in low-pressure applications of Isopentane (55.6% of η_C at *Δp = 5 bar*) or Isobutane (55% of η_C at *Δp = 10 bar*). Although the specific power typically rises with increasing pressure change (see Figure 19), such fluids are interesting for applications in which larger pressure changes are a concern.

Mixture working fluids

The potential efficiency is restricted by thermodynamic limitations to the maximum possible regeneration efficiency. For pure fluids, large temperature plateaus in the cumulative enthalpy curves associated with evaporation at p_{high} and condensation at p_{low} are responsible for relatively inefficient regeneration (i.e. large distances of these curves in the T-H-Diagram, see Figure 21a).

Mixtures with sufficiently different boiling points, in which phase transition occurs within a temperature range, can be applied to reduce this effect significantly (Figure 21b). From a set of mixtures under investigation, the best results were found for a mixture of propane and pentane with 35 wt-% of propane. The mixture is indicated in Figure 20 by a star-shaped marker. At $T_H = 100°C$, the maximum efficiency of 58.1% of η_C is found at Δp of only 5 bar, which is the highest efficiency of all investigated fluids at that temperature constellation. At higher heat source temperatures, the advantage of mixtures is less pronounced. Although the mixture is the superior working fluid at $\Delta p < 25$ *bar*, propane with a higher-pressure change offers better energy conversion efficiency.

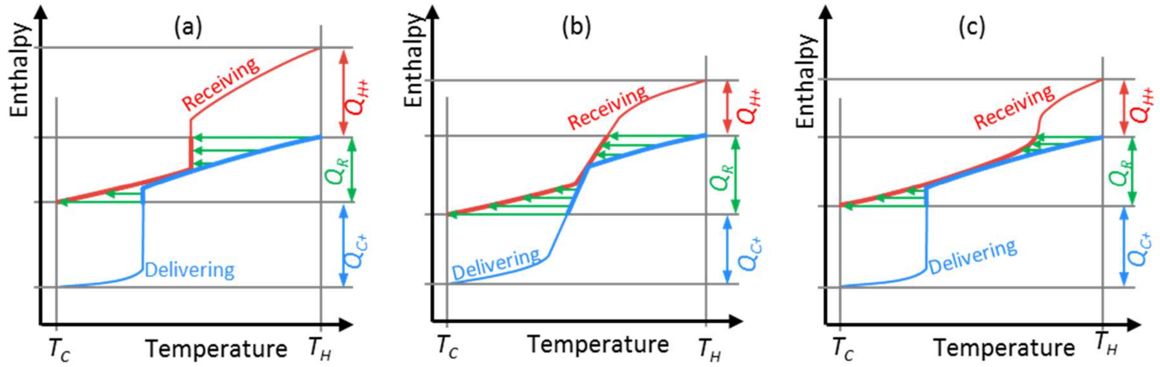

Figure 21: Typical curves of the cumulative enthalpies for a subcritical phase-changing working fluid (a), a mixture in phase-change operation (b) and a supercritical working fluid with ph > pcrit (c).

Supercritical working fluids

While the maximum pressure in the engine was restricted to subcritical pressures in the previous sections, supercritical operation is another option to increase the regeneration potential. If the maximum cycle pressure exceeds the critical pressure of the respective working fluid, the temperature plateaus of the cumulative enthalpy disappear. Instead, the fluid transits continuously from a liquid-like state to a gas-like (supercritical) state when being heated. Consequently, the cumulative enthalpy curves can approach closer (Figure 21c). This characteristic enables very high efficiencies above 70% of Carnot efficiency, see Figure 22. At lower hot space temperatures ($T_H = 100°C$, $T_H = 150°C$), refrigerant R32 shows very promising results, whereas at higher temperatures ($T_H = 200°C$, $T_H = 300°C$), propane was found to be the most favourable working fluid, out of all working fluids under consideration. Maximum efficiencies for operation with supercritical fluids are found at pressure changes larger than 50 bar, which implies additional requirements to the materials and equipment used for real engines of this type. If such high pressures are feasible in the operational environment of an IE engine, supercritical working fluids display the best characteristics in terms of efficiency. Moreover, they offer exceptional specific power since much larger pressure changes can be realised as compared to subcritical fluids.

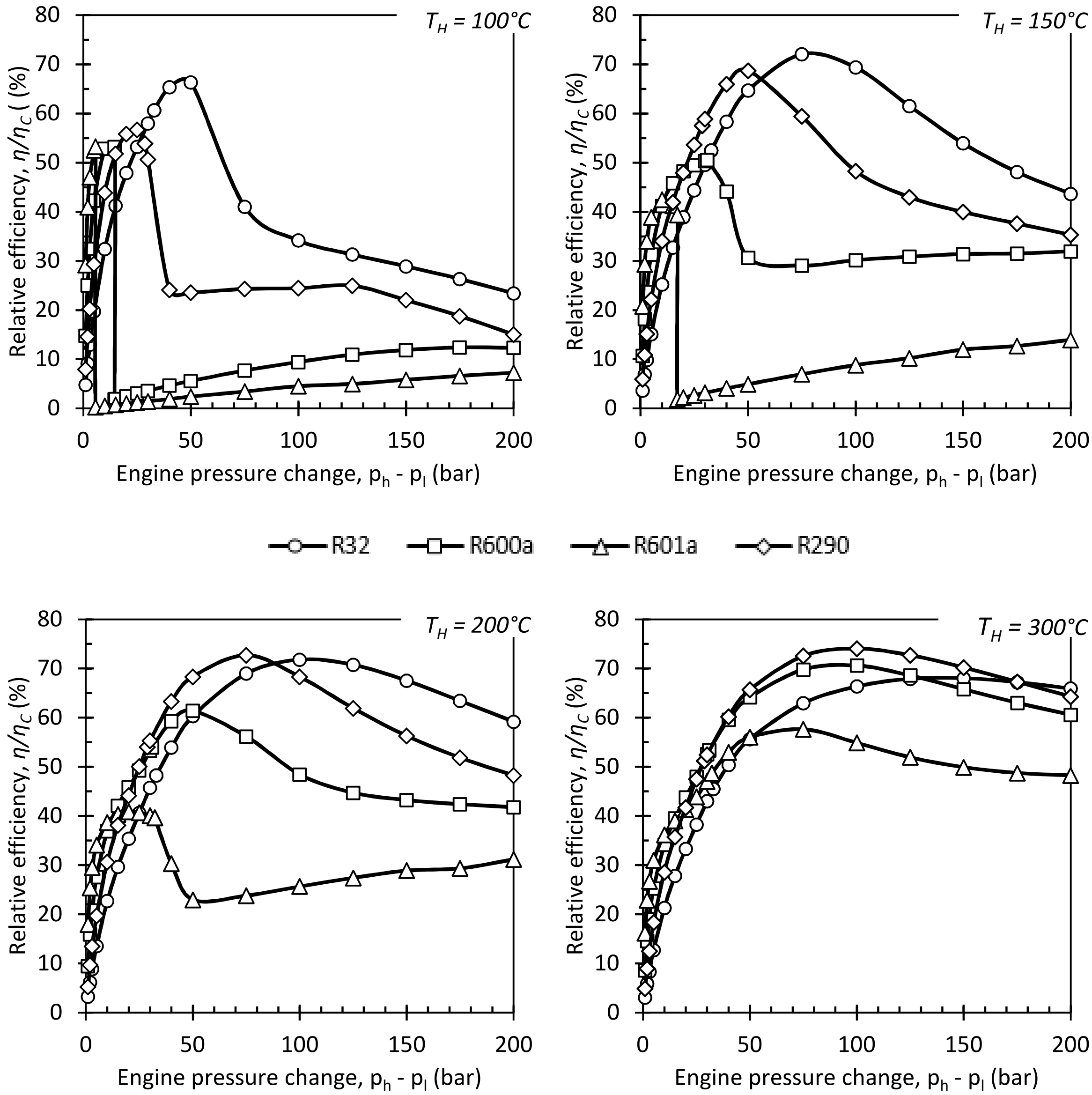

Figure 22: Simulated maximum energy conversion efficiencies at TC = 40°C and different values of TH in dependence on the engine pressure change and in relation to the respective Carnot efficiency with extension to supercritical pressures.

3.7. Concluding remarks

A thermodynamic model of isobaric expansion engines was extended to capture the effects of internal volumes and pressure drop caused by inevitable heat exchanger equipment on the performance of such engines. In the conceptual study, a PCHE which is a special type of compact heat exchanger was selected and used in the IE engine system design. In a preliminary design approach, the size and frictional pressure drop of such heat exchangers were estimated as functions of the desired recuperation efficiency for a set of different channel diameters and maximum fluid velocities inside the channels.

An investigation of the individual influences of dead volumes and pressure drop indicated that the detrimental influence of dead volumes is less pronounced when the compressibility of the working fluid is low. Although the use of dense working fluids mitigates the problem of dead volumes known in the design of gas-phase Stirling engines, significant efficiency losses may occur if the dead volumes are too high. Frictional pressure drop is of lower importance as compared to dead volumes, but it should nevertheless be carefully taken into account in the design of IE engines.

A study of the combined effect of efficient recuperative heat transfer and the associated dead volumes (as internal volumes of the heat exchangers) and pressure drop on the thermal efficiency affirmed the importance of the application of very compact heat exchangers. Heat exchanger channels with very small dimensions (d <= 1 mm) should be chosen to avoid too bulky and long heat exchanger units, particularly in terms of the residence-time to cycle-time ratio. Heat exchanger channels with bigger dimensions and lower surface density, consequently causing larger dead volumes, were shown to decrease the efficiency remarkably. Moreover, the results indicated that the most efficient recuperation does not necessarily result in the maximum efficiency. In many cases, a drop off in efficiency was observed when the desired regeneration efficiency was too high. This can be attributed to a disproportionate increase of required heat exchanger length (and, accordingly, pressure drop) for highly effective recuperation (ΔTmin << 5 K).

Ultimately, the potential effects of recuperation were studied for three different grades of heat sources (TH = 80, 120 and 200°C). It was found that the positive effect of recuperation is most pronounced at high temperatures of the heat source, whereas in low-temperature applications, non-recuperative efficiencies could already reach up to 45% of Carnot efficiency. At higher temperatures, relative efficiencies of up to 65% can be obtained.

In conclusion, this work demonstrates the great potential of IE engines as a technology for conversion of heat to mechanical energy, particularly in small-scale and/or ultra-low-temperature applications. The great importance of efficient regeneration at higher heat source temperatures was emphasised. Future work in this field will be devoted to an experimental validation of the results obtained. Furthermore, the fluid flow in IE engines will be investigated, both experimentally and numerically, aiming at improvement of the simplified methods applied in this report, in order to develop a solid thermal design strategy for heat exchangers in IE engines.

A comprehensive study of several potential working fluids, including subcritical and supercritical fluids as well as mixtures, for novel-type IE engines has been performed. These results were obtained using a thermodynamic model in order to predict energy conversion efficiency and specific power reliant on thermodynamic properties and operational parameters such as temperature and pressure levels. Operation beyond the critical pressure, i.e. $p_{high} > p_{crit}$, delivers the highest efficiencies in combination with large specific power. The highest efficiency is explained by similar courses of the cumulative enthalpies, enabling to effectively regenerate heat throughout the cycle. A potential drawback of this type of operation is the relatively high pressure, which might be problematic in view of the necessary equipment. Subcritical, two-phase operation is a way to obtain relatively high efficiencies at pressure changes lower than 30 bar. At ultra-low heat source temperatures, high efficiency can be found operating at even lower pressures.

In conclusion, it has been demonstrated that novel-type heat engines using dense working fluids offer a great new opportunity for different applications of heat valorisation, whether it be for electric power generation or heat-driven pumps and compressors.

4. ECT Engine-pump design and manufacturing

4.1. Design of the engine components

Based on the results achieved from the development of previous small power IE engines, and from the modelling results from Task 3.4.1, a novel, scalable IE engine-pump with external heat exchangers was designed. In contrast to the previously developed IE engines the new machine is scalable up to several MW.

Generally, the engine design was focused on finding a compromise between low heat losses, high heat exchange rates, low pressure drops, small dead volumes, high heat capacity of the solid phase and small footprint.

Heat exchangers (heater, regenerator and cooler combination) are the heart of an engine. The main requirement of the heat exchanger is to have as small as possible dead volume and high endurance i.e. an ability to sustain high amplitude pressure variations. Literally all types of heat exchangers were examined as the possible candidates:

- Spiral
- Brazed plate
- Welded and semi-welded plate
- Gasketed plate
- Pillow plate
- Shell and tubes
- Made by additive manufacturing (3D printing)
- Printed circuit diffusion bonded

All flat plate heat exchangers shown very low endurance limits i.e. inability to resist the medium and high amplitude pressure variations typical of IE engine. Such low endurance is caused by an excessive compliance/flexibility of the thin metal (stainless steel) plates under influence of the pressure variations. The reason is the state-of-the-art technical manufacturing level, which permits the minimum possible channel height of about 3 mm. A relatively thin, flexible metal wall of such a channel can “play” during pressure variations. Such a play results in wear and tear of the plate contact areas and larger channels may lead to an excessively high dead volume. In addition, manufacturing of bespoke brazed/welded plate and spiral heat exchangers is expensive. These types of heat exchangers are low cost in today’s market, but only where mass produced. Generally, the channel size of the plate heat exchangers is getting less and less every several years. At certain channel sizes, issues due to excessive compliance and dead volume could be resolved.

The pillow plate heat exchangers can resist the pressure variations and might be used for some particular cases/applications. But, generally, they are very sensitive with respect to heating and cooling agent distribution.

Conventional welded shell and tube heat exchangers were excluded from the consideration due to very high dead volumes, especially the internal volumes of headers and a poor heat exchanging area to weight ratio.

The heat exchangers made using one of many additive manufacturing processes seem to be a very attractive solution. They can be made from any materials with any suitable combination of channel size and metal thickness. The manufacturing price drops down every year, but manufacturers cannot guarantee the required material density or safety levels. In fact, the development of such a heat exchanger today requires a separate R&D project. Nevertheless, additive manufactured heat exchangers in the near future may be seen as a very promising candidate.

Printed circuit diffusion bonded heat exchangers (PCHE) were recognized as the most promising candidates today. They can be made on request by several companies from a variety of materials (aluminum, steel, alloys). They can withstand the combination of very high temperatures and pressures, which covers any possible operating area of IE engines. Manufacturing prices also drop every year. However, experimenting with PCHEs by ordering many different types with different channel geometries and wall thicknesses is very expensive.

As a result, a decision was made to design a pseudo-PCHE heat exchanging structure imitating a real PCHE. In total, four combinations of heater, regenerator and cooler of different dimensions and materials (two from aluminum and two from stainless steel) were made from commercially available cheap elements.

All the necessary production drawings of the engine were produced and the engine parts were manufactured by a specialized machine-building company - TenHeggeler Machinefabriek, Hengelo, The Netherland (http://www.tenheggeler.com/tenheggeler.htm).

The new scalable engine-pump was assembled and equipped with heating, cooling, measuring and control equipment.

Experimental studies of the different heat exchangers and engine-pump as whole are now in progress.

4.2. Production drawings of the pressure converting units

In order to study the performance of the engine-pump three types of engine loads – pressure converting units – were designed and built. The first pressure converting unit operates as a pump driven by the engine whereas the two others, the so-called indicators, were designed in order to study quantitatively engine performance. They are convenient to measure the displacement of the liquid working fluid from the engine cylinder. In addition, all the pressure converting units are used for selection of materials and pistons seals that are compatible with the engine working fluid and characterized by low frictional losses.

Figure 23 and Figure 24 show 3D views of the pump and 40 mm indicator.

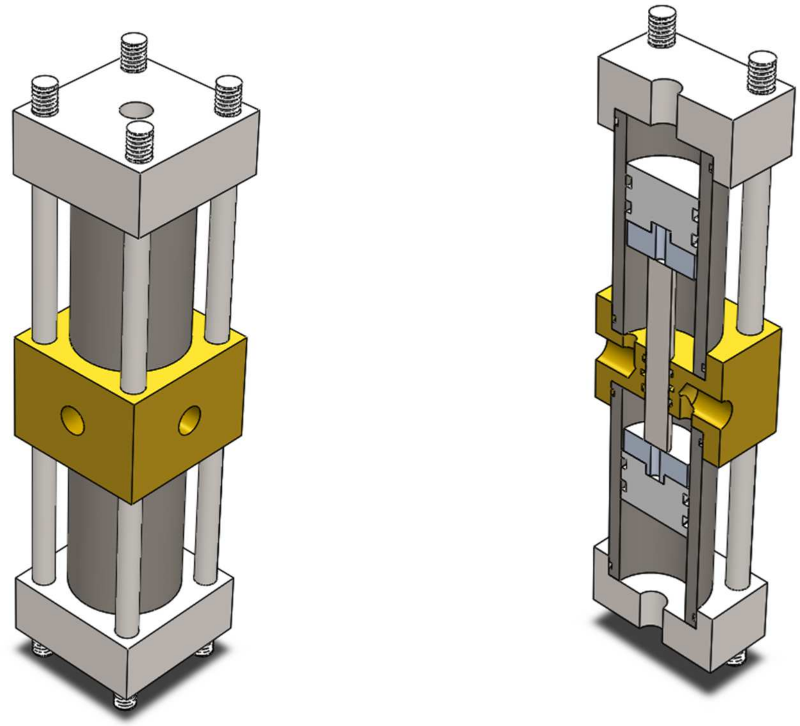

Figure 23: Pressure converting unit: pump.

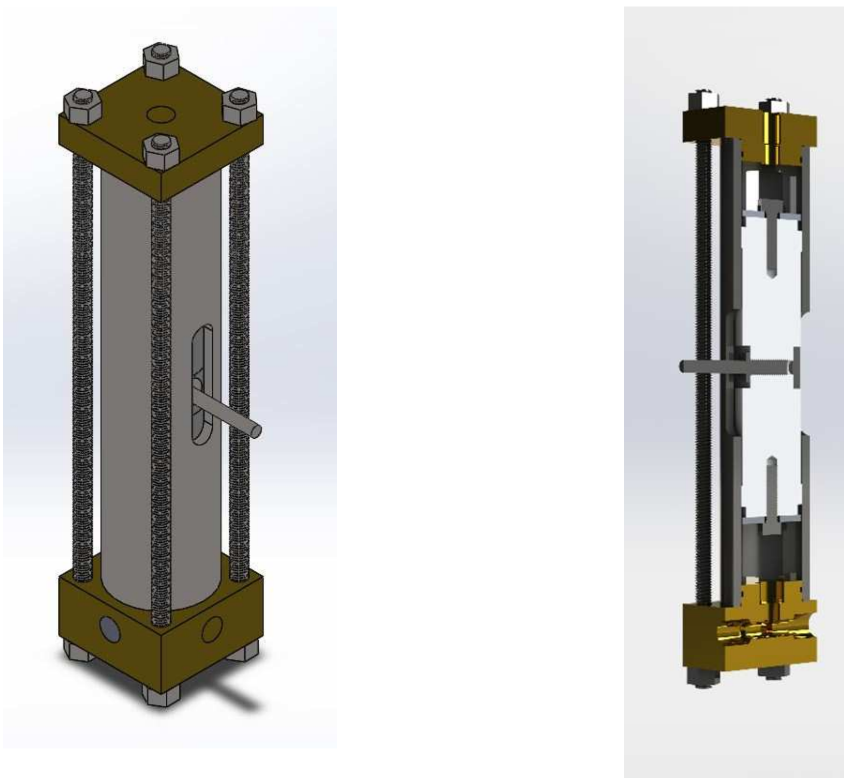

Figure 24: Pressure converting unit: 40 mm indicator.

Production drawings of the pressure converting units are presented in Annexes A, B, and C.

4.3. Engine-pump standard components

In addition to the designed parts (heat exchangers, displacer, engine body, etc.) many standard parts such as sealing rings, connectors, tubing, fittings, etc. were selected and ordered. Figure 25 shows a part of the engine test set up to explain some of the standard components.

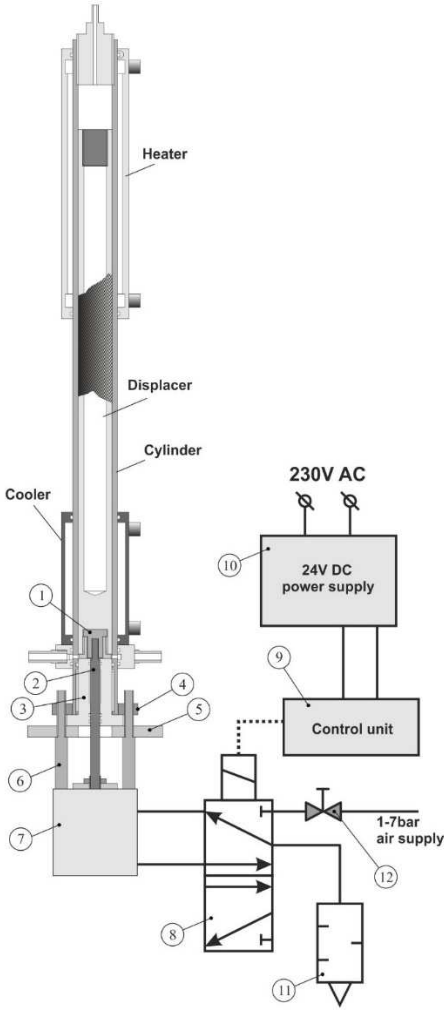

Figure 25: Part of the engine test set up with the small-scale engine.

The standard components include among others:

1. Double Acting Pneumatic Air Cylinder, ELE ALL. SDA63mm*45mm / 63mm bore, 45mm stroke. 0.1- 0.9 MPa., Number 7, Figure 25.
2. Solenoid valve, AirTAC. Model 4V210-08. Pressure 0.15-0.8 MPa. Number 8, Figure 25.
3. Control unit, OMRON H3YN-2 Timer, DC 24V. Number 9, Figure 25.
4. Power supply, TRACO POWER, TMP 15124C. Input 100-240 VAC/380mA max. Output 24 VDC/ 625 mA. Number 10, Figure 25.
5. Silencers. Number 11, Figure 25.
6. Throttling valve, Sun Rise, Tong Chen, RE-02. Number 12, Figure 25.
7. Pressure transmitters PT, Sendo JF302 5MPa gauge, Ninghai Sendo Sensor Co., Ltd, Hangzhou, China with 0.5% accuracy and 4 ms response time.

8. Manometers, Empeo, 6 MPa with 1.6% accuracy.
9. 12 bits PicoLog 1000 data acquisition system with 1 MS/s sampling rate.
10. 1 mm and 0.5 mm shielded K-types thermocouples, pre-calibrated in the range of 0–100 °C.
11. Multiple seals, see the production drawings, Annexes A, B, C. Annex D contains an example of the ordered and studied seals.

All the transmitters had 4–20 mA output to avoid any influence of cable lengths.

The experimental set-up includes both static and dynamic seals of the tubes and pistons which are very important for robust and efficient engine operation. Static seals (O-rings) were used for sealing of the cylinder cover and the heat exchanger tubes. Dynamic seals were used for sealing of the displacer and the rod of the linear actuator.

IE engine can use a great variety of working fluids. The most logical candidates are hydrocarbons and especially their mixtures. Most of the hydrocarbons, even with oil addition, permit a very broad range of polymer sealing materials. PTFE-based ones are the most practicable of them due to a very low frictional losses (i.e. a high mechanical efficiency) and wear. For static sealing at higher temperatures (up to 200 °C), FKM-based materials (Viton etc.) are one of the best solutions.

Unfortunately, the fluorinated hydrocarbons exclude the use of both PTFE and FKM based seals. Only NBR and EPDM based materials showed an acceptable operational capability, although some swelling was detected. FKM and PTFE demonstrated an unacceptable, severe swelling; sizes of the parts changed so significantly, that they could be removed only by hammering.

Such problems in the future might lead to a review of working fluid selection.

5. Conclusions

In the course of the theoretical research, a thermodynamic model of regenerative displacer-type heat engines suitable for arbitrary working fluids and arbitrary engine cycles was developed. Also, thermodynamic limits on the heat regeneration in case of non-ideal fluids were studied and used for evaluation of the heat regeneration efficiency.

Performance of an IE engine-pump was studied theoretically at various heat source temperature and pressure head to observe the impact of working fluids and process conditions on energy conversion efficiency and power density.

As part of D3.5 widely used refrigerant R134a was selected as working fluid at the current stage of the engine development. In addition, theoretical results show that mixtures of working fluids could be beneficial for the cycle energy efficiency and engine power density.

Based on the results achieved from the development of previous small power IE engines, and from the modelling results from Task 3.4.1, a novel, scalable IE engine-pump with external heat exchangers was designed.

All the necessary production drawings of the engine have been produced and engine parts manufactured by a specialized machine-building company. In addition to the designed parts (heat exchangers, displacer, engine body, etc.) many standard parts such as sealing rings, connectors, tubing, fittings, etc. were selected and ordered.

In total, four combinations of heater, regenerator and cooler of different dimensions and materials (two from aluminium and two from stainless steel) were made from commercially available cheap elements.

The new scalable engine-pump was assembled and equipped with heating, cooling, measuring and controlling equipment. Experimental studies of different heat exchangers and engine-pump designs are in the progress.

References

[1] M. Glushenkov y A. Kronberg, Heat to mechanical energy converter. PCT/EP2012/064094, International Publication Number WO 2014/012586 A1., 18.07.2012.

[2] M. Glushenkov, M. Sprenkeler y A. Kronberg, «Regenerative Heat to Mechanical Energy Converter with Dense Working Fluid. Proceedings of the 16th International Stirling Engine Conference,» de *177-186. ISSN 2409-0387*, Bilbao, Spain, 24 – 26 September 2014.

[3] M. Glushenkov, A. Kronberg, T. Knoke y E. Kenig, « Isobaric Expansion Engines: New opportunities in energy conversion for heat engines, pumps and compressors,» *Energies ,* vol. 1, nº 11, pp. 154-175, 2018.

[4] R. Sier, John Fox Jennens Malone: The Liquid Stirling Engine, John Fox Jennens Malone., 2007.

[5] G. Walker, Stirling Engines., Oxford: Clarendon Press, 1980.

[6] X. Chen, B. Xu y L. Liu, «Nanoscale fluid mechanics and energy conversion,» *ASME Applied Mechanics Reviews,* vol. 5, nº 66, pp. 050803-1 - 050803-17, 2014.

[7] G. Angelino y C. Invernizzi, «Real gas effects in Stirling engines,» de *Proceedings of the Intersociety Energy Conversion Engineering Conference. Volume 1, pp 69-75.*, 2000.

[8] G. Walker y J. Senft, Free Piston Stirling Engines., Berlin/Heidelberg, Germany: Springer, 1985.

[9] I. Kolin, Thermodynamics Atlas: The Evolution of the Heat Engine., London, UK: Longman, 1967.

[10] M. Glushenkov, M. Sprenkeler, A. Kronberg y V. Kirillov, «Single-piston alternative to Stirling engines.,» *Applied Energy,* nº 97, pp. 743-748, 2012.

[11] W. Martini, Stirling Engine Design Manual, U.S. Department of Energy, Office of Conservation and Solar Applications, Division of Transportation Energy Conservation, 1978.

[12] M. Bianchi y A. De Pascale, «Bottoming cycles for electric energy generation: Parametric investigation of available and innovative solutions for the exploitation of low and medium temperature heat sources,» *Applied Energy,* vol. 5, nº 88, pp. 1500-1509, 2011.

[13] S. Lemmens, «Cost engineering techniques and their applicability for cost estimation of Organic Rankine Cycle systems,» *Energies,* vol. 7, nº 9, p. 485, 2016.

[14] F. Heberle y D. Brüggemann, «Thermo-economic evaluation of Organic Rankine Cycles for geothermal power generation using zeotropic mixtures,» *Energies ,* vol. 3, nº 8, pp. 2097-2124, 2015.

[15] K. Wang, S. Sanders, S. Dubey, F. Choo y F. Duan, «Stirling cycle engines for recovering low and moderate temperature heat: A review,» *Renewable and Sustainable Energy Reviews,* nº 62, pp. 89-108, 2016.

[16] T. Mancini, P. Heller, B. Butler, B. Osborn, W. Schiel, V. Goldberg, R. Buck, R. Diver, C. Andranka y J. Moreno, «Dish-Stirling systems: An overview of development and status,» *Journal of Solar Energy Engineering,* vol. 2, nº 125, pp. 135-151, 2003.

[17] H. Hachem, R. Gheith, F. Aloui y S. Ben Nasrallah, «Technological challenges and optimization efforts of the Stirling machine: A review,» *Energy Conversion and Management,* nº 171, pp. 1365-1387, 2018.

[18] G. Simader, R. Krawinkler y G. Trnka, «Micro CHP systems: state-of-the-art. Final Report.,» Delivrable 8 (D8) of Green Lodges Project (EIE/04/252/S07.38608), Österreichische Energieagentur, Austrian Energy Agency, 2006.

[19] K. Makhkamov y D. Ingram, «Analysis of the working process and mechanical losses in a Stirling engine for a solar power unit,» *Journal of Solar Energy Engineering,* vol. 2, nº 121, pp. 121-127, 1999.

[20] B. Kongtragool y S. Wongwises, «Thermodynamic analysis of a Stirling engine including dead volumes of hot space, cold space and regenerator,» *Renewable Energy,* vol. 3, nº 31, pp. 345-359, 2006.

[21] P. Puech y V. Tishkova, «Thermodynamic analysis of a Stirling engine including regenerator dead volume.,» *Renewable Energy,* vol. 2, nº 36, pp. 872-878, 2011.

[22] S. Alfarawi, R. Al-Dadah y S. Mahmoud, «Influence of phase angle and dead volume on gamma-type Stirling engine power using CFD simulation,» *Energy Conversion and Management,* nº 124, pp. 130-140, 2016.

[23] V. Bush, «Apparatus for Compressing Gases». U.S. Patente Patent 2, 17 July 1935.

[24] W. Martini, «Stirling Cycle Amplifying Machine». U.S. Patente Patent 3,513,659, 26 May 1971.

[25] F. Huffman, «Tidal Regenerator Heat Engine». U.S. Patente Patent 3,657,877, 01 February 1971.

[26] K. Hagen, F. Huffman y A. Ruggles, «Expansion Tidal Regenerator Heat Engine». U.S. Patente Patent 3,986,360, 06 June 1975.

[27] A. Organ, The Regenerator and the Stirling Engine, Hoboken, NJ, USA: John Wiley & Sons, 1997.

[28] J. Hesselgreaves, Compact Heat Exchangers: Selection, Application, Design and Evaluation, Pergamon, Turkey: Elsevier, 2001.

[29] S. Kakaç, H. Liu y A. Pramuanjaroenkij, Heat Exchangers: Selection, Rating, and Thermal Design, Boca Raton, FL, USA: CRC Press, 2012.

[30] B. Haynes y A. Johnston, «High-effectiveness micro-exchanger performance,» de *Proceedings of the AIChE 2002 Spring National Meeting*, New Orleans, LA, USA., 2002.

[31] Q. Li, G. Flamant, X. Yuan, P. Neveu y L. Luo, «Compact heat exchangers: A review and future applications for a new generation of high temperature solar receivers,» *Renewable and Sustainable Energy Reviews,* pp. 4855-4875, 2011.

[32] I. Kim, X. Zhang, R. Christensen y X. Sun, «Design study and cost assessment of straight, zigzag, S-shape, and OSF PCHEs for a FLiNaK–SCO2 Secondary Heat Exchanger in FHRs,» *Annals of Nuclear Energy,* nº 94, pp. 129-137, 2016.

[33] T. Knoke, E. Kenig, A. Kronberg y M. Glushenkov, «Model-based analysis of novel heat engines for low-temperature heat conversion,» *Chemical Engineering Transactions,* nº 57, pp. 499-504, 2017.

[34] B. Dodge, Chemical Engineering Thermodynamics, London/New York, UK/USA: McGraw-Hill, 1944.

[35] R.K. Shah, D.P. Sekulić, Fundamentals of Heat Exchanger Design, John Wiley & Sons, Hoboken, NJ, 2003 https://doi.org/10.1002/9780470172605

[36] V. Gnielinksi, «Ein neues Berechnungsverfahren für die Wärmeübertragung im Übergangsbereich zwischen laminarer und turbulenter Rohrströmung (in German). Forschung im Ingenieurwesen,» *Engineering Research,* nº 61, pp. 240-248, 1995.

[37] P. Konakov, «A new correlation for the friction coefficient in smooth tubes (Orig. in Russian),» *Reports of the Academy of Sciences of the USSR,* nº 51, pp. 503-506, 1946.

[38] D. Steiner y J. Taborek, «Flow boiling heat transfer in vertical tubes correlated by an asymptotic model,» *Heat Transfer Engineering,* vol. 2, nº 13, pp. 43-69, 1992.

[39] J. Thome, V. Dupont y A. Jacobi, «Heat transfer model for evapouration in microchannels. Part I: presentation of the model,» *International Journal of Heat and Mass Transfer,* Vols. %1 de %214-16, nº 47, pp. 3375-3385, 2004.

[40] H. Müller Steinhagen y K. Heck, «A simple friction pressure drop correlation for two-phase flow in pipes,» *Chemical Engineering and Processing,* nº 20, pp. 297-308, 1986.

[41] R. Numrich y J. Müller, Filmwise Condensation of Pure Vapours, Heidelberg, Germany: VDI Heat Atlas, 2010.

[42] A. Cavallini, L. Doretti, M. Matkovic y L. Rossetto, «Update on condensation heat transfer and pressure drop inside microchannels,» *Heat Transfer Engineering,* vol. 4, nº 27, pp. 74-87, 2006.

[43] K. Nikitin, Y. Kato y L. Ngo, «Printed circuit heat exchanger thermal–hydraulic performance in supercritical CO2 experimental loop.,» *International Journal of Refrigeration,* vol. 5, nº 29, pp. 807-814, 2006.

[44] «Vacuum Process Engineering,» 2018. [En línea]. Available: http://vpei.com/wp-content/uploads/Hex-Core-Layered.jpg. [Último acceso: 13 November 2018].

[45] C. Hargreaves, The Philips Stirling Engine, Amsterdam, The Netherlands: Elsevier, 1991.

[46] E. Lemmon, I. Bell, M. Huber y M. McLinden, *NIST Standard Reference Database 23: Reference Fluid Thermodynamic and Transport Properties-REFPROP, Version 10.0,* National Institute of Standards and Technology, Standard Reference Data Program, 2018.

Annexes

List of Annexes:

- Annex A. Production drawings of the pump.
- Annex B. Production drawings of the 16-32 mm indicator.
- Annex C. Production drawings of the 40 mm indicator.
- Annex D. Sealing rings.

Annex A. Production drawings of the pump.

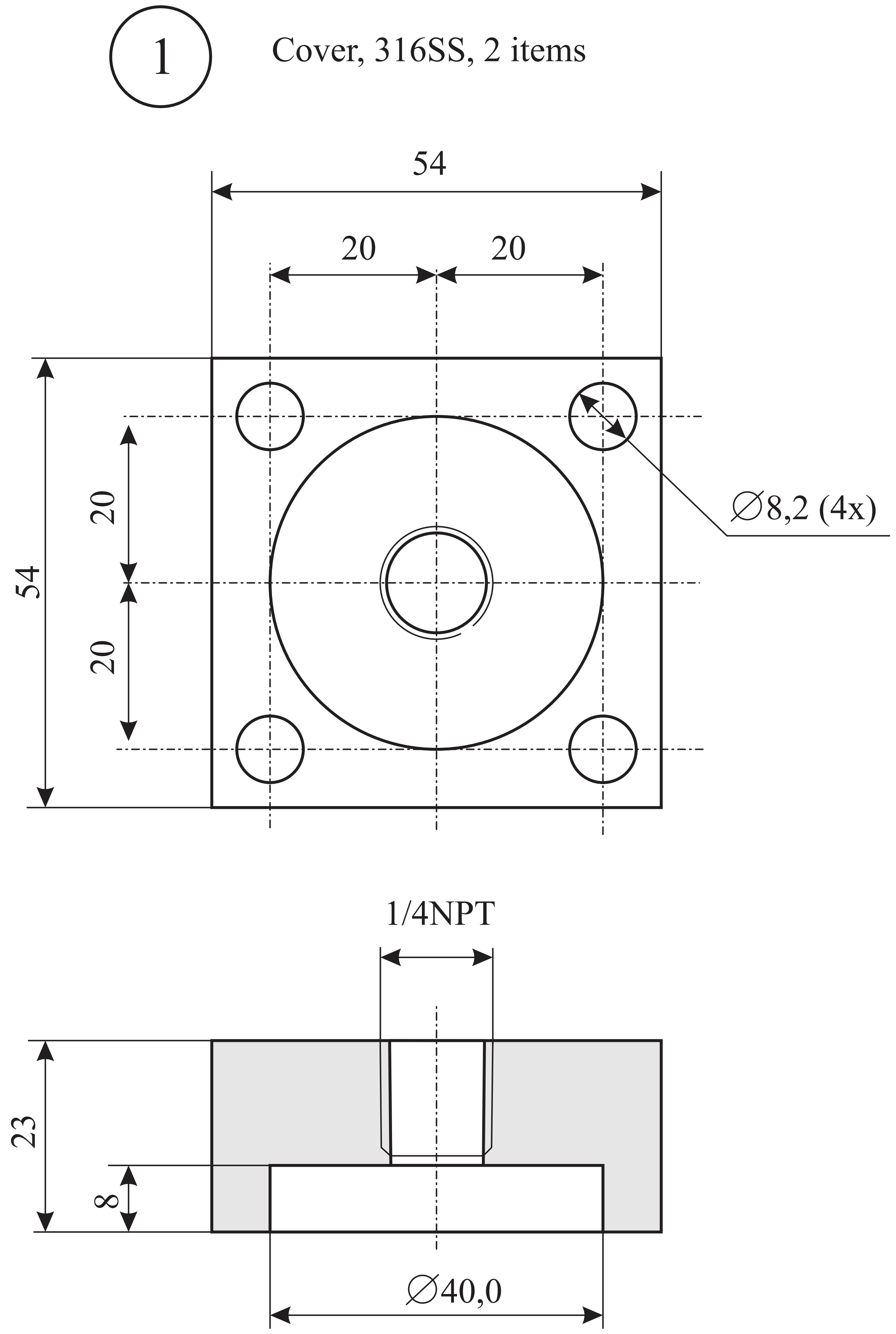
1
Cover, 316SS, 2 items
54
20
20
54
20
20
∅8,2 (4x)
1/4NPT
23
8
∅40,0

2 cylinder, 316SS, 2 items

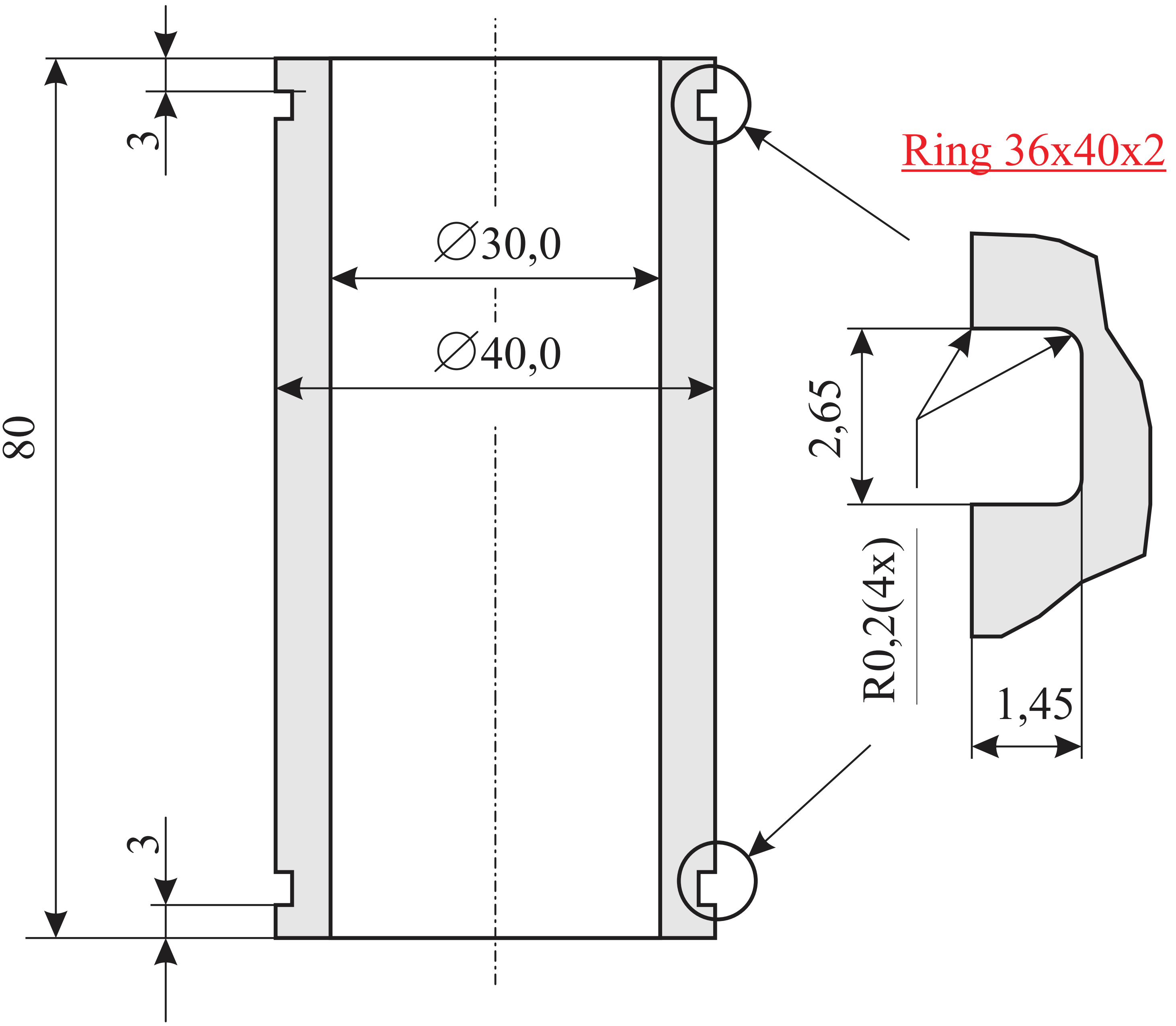

3

piston, bronze, 2 items

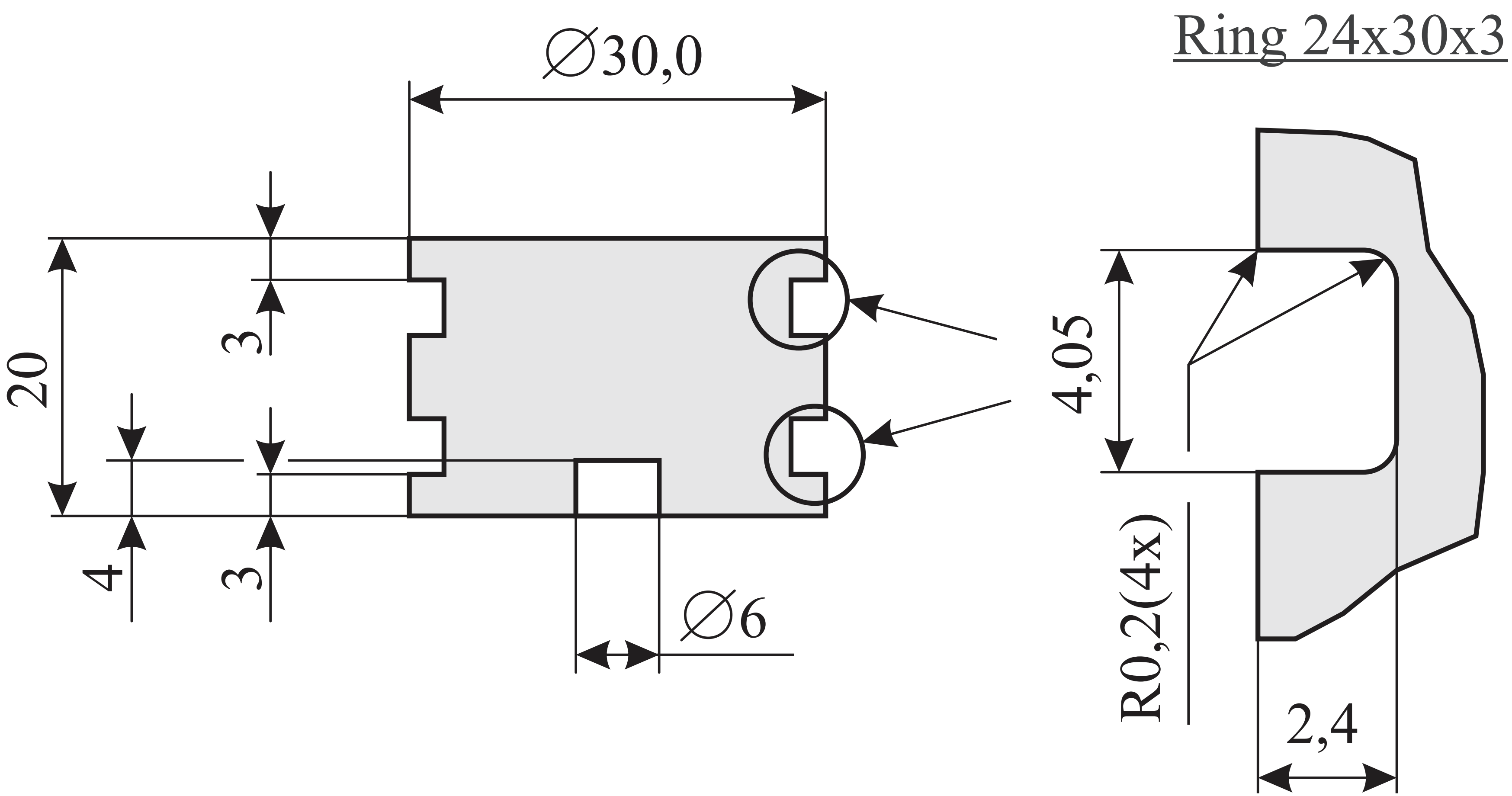

4

Valve head 316SS, 1item

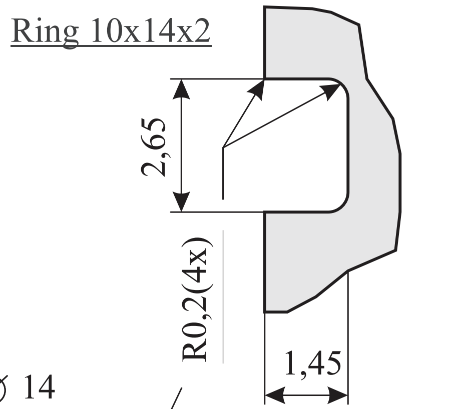

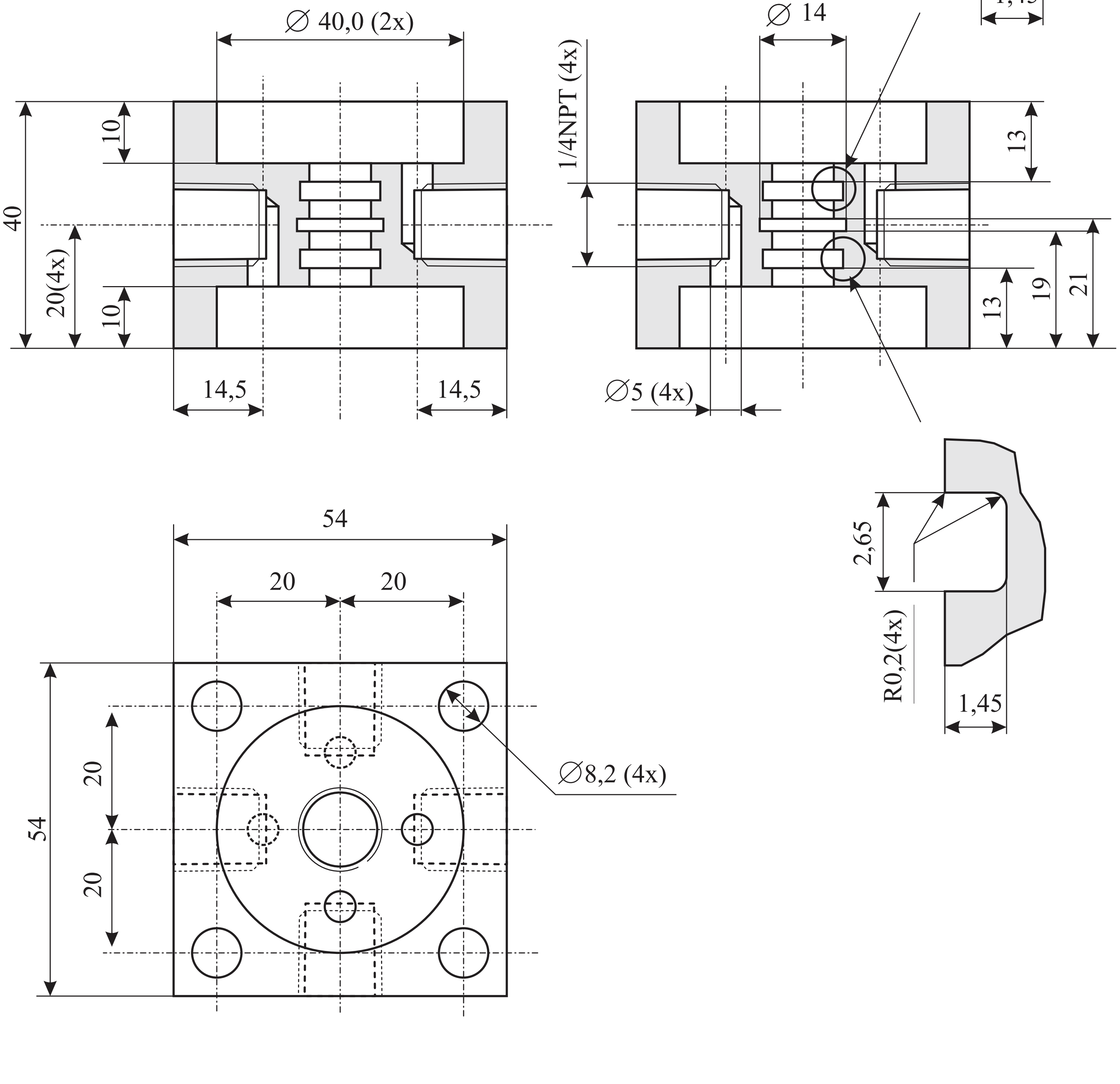

5

Rod, 1 item, 316SS

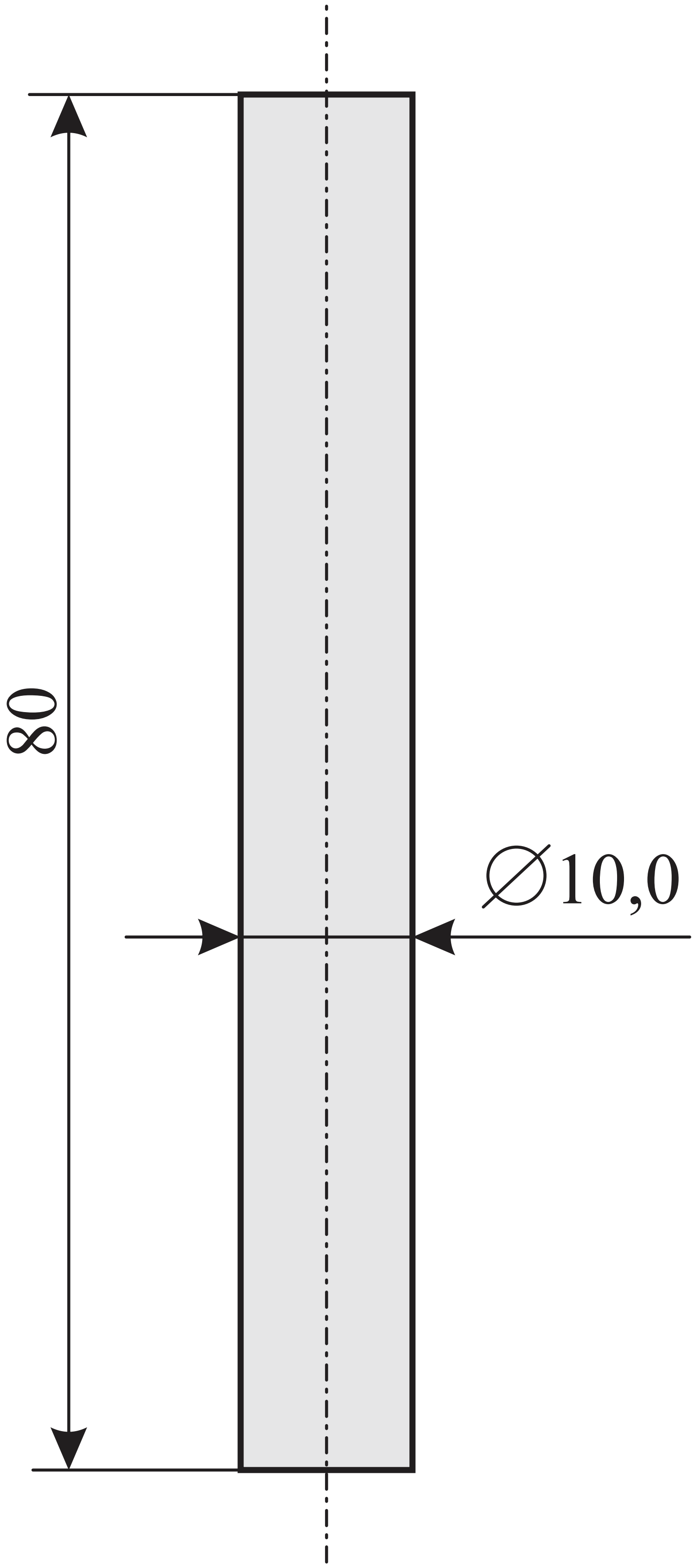

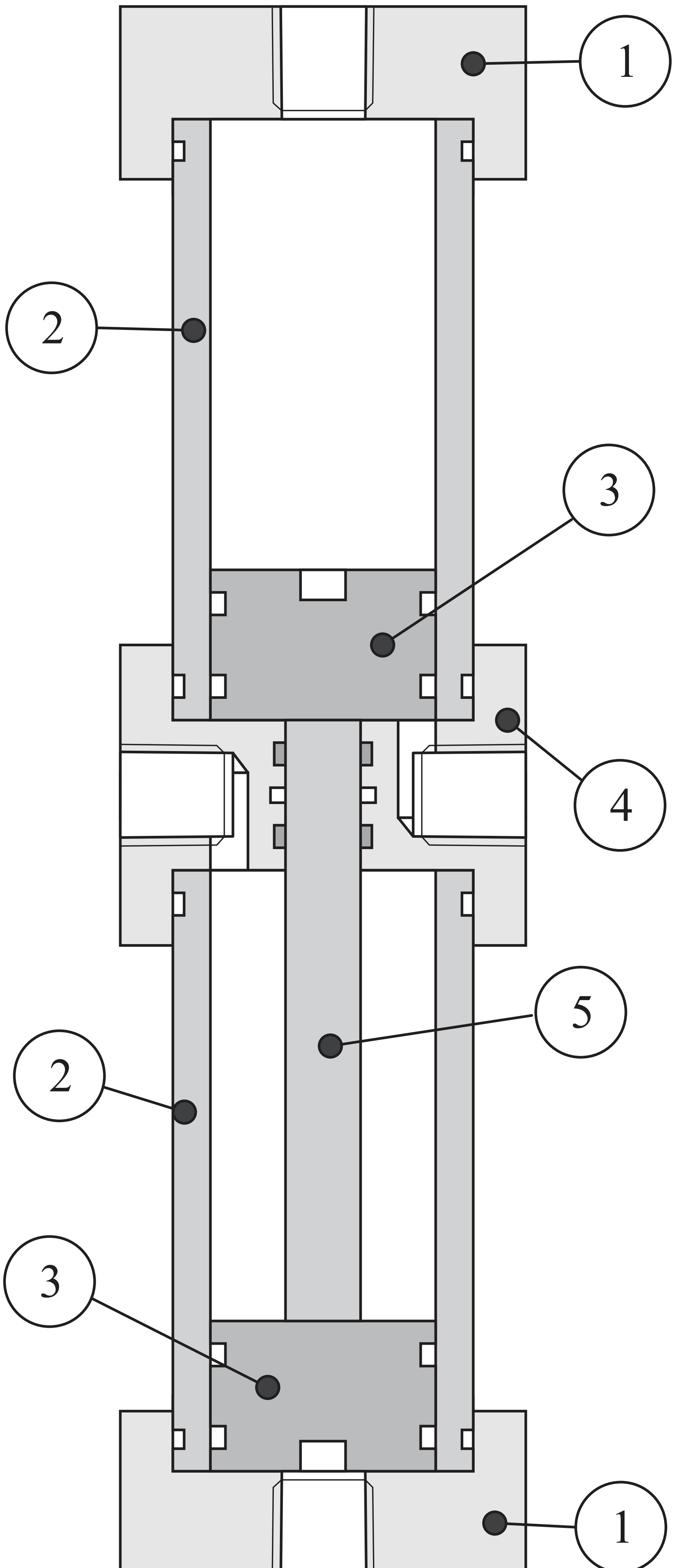
1
2
3
4
5
2
3
1

Annex B. Production drawings of the 16-32 mm indicator

1 Lower cover, steel, bronze,1 item

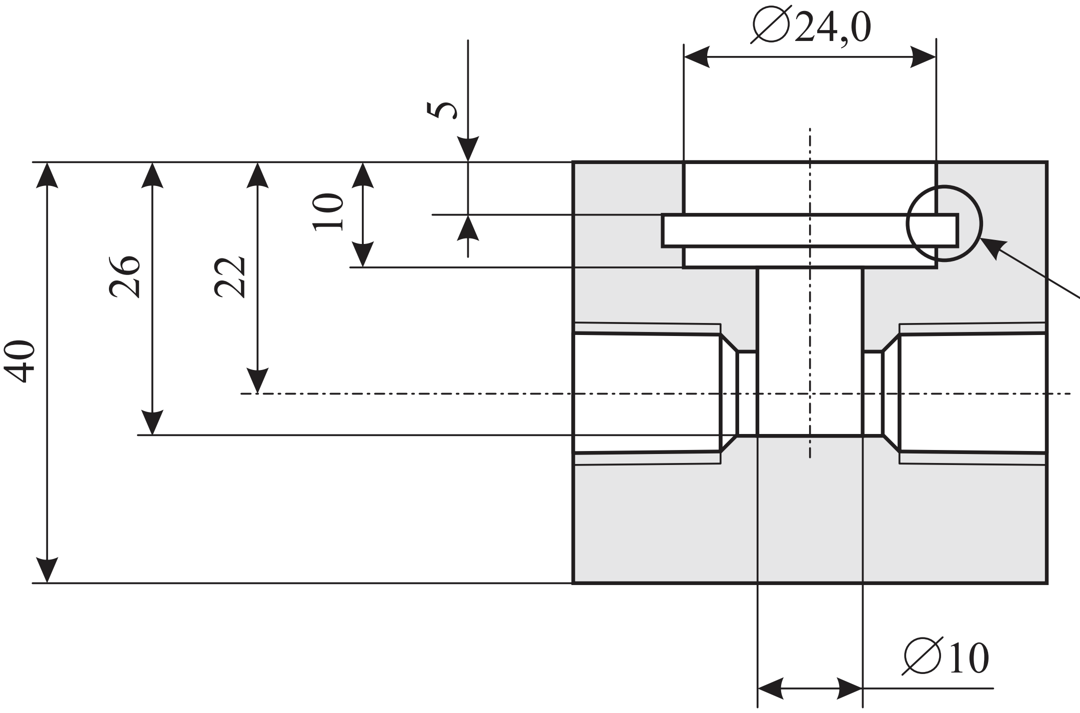

Ring 24x28x2

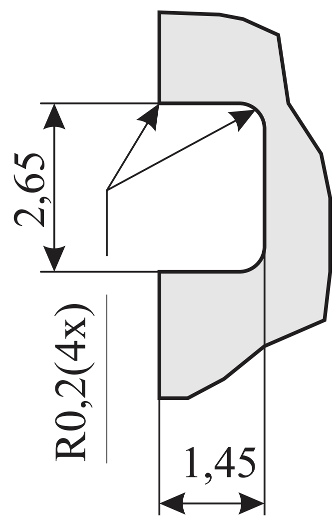

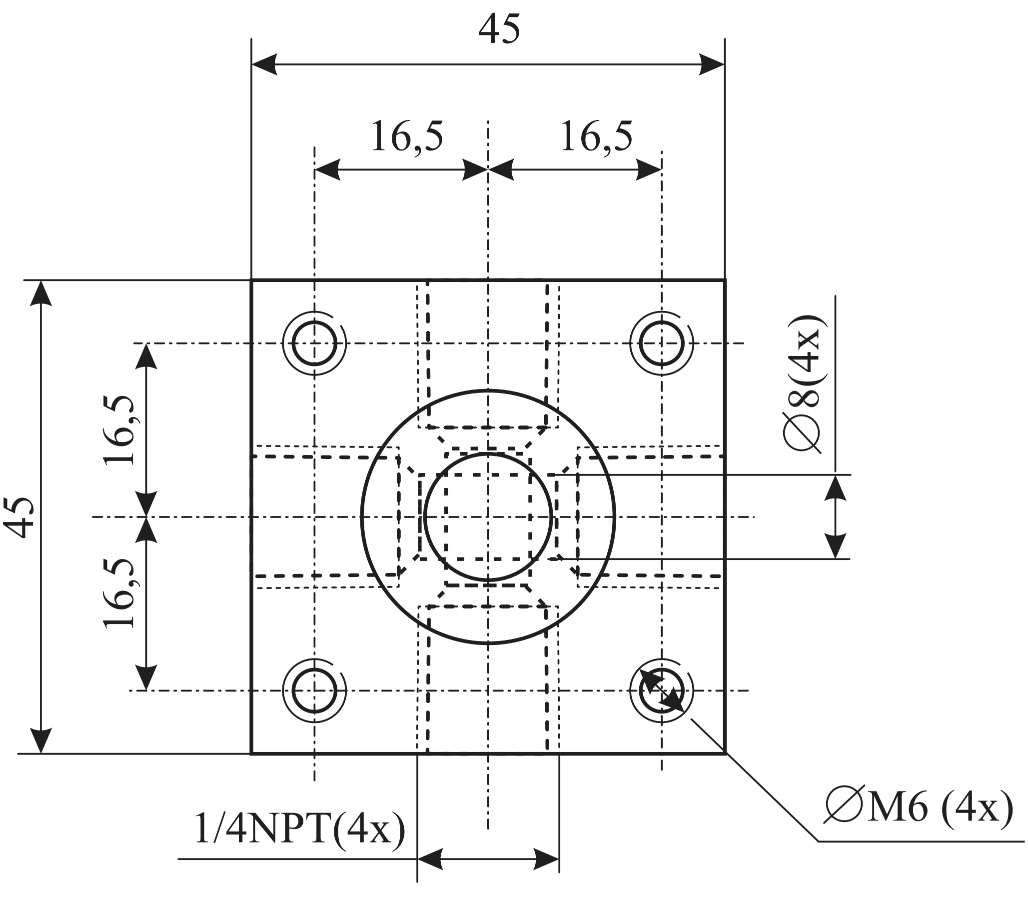

2 piston, carbon-filled teflon, 1 item

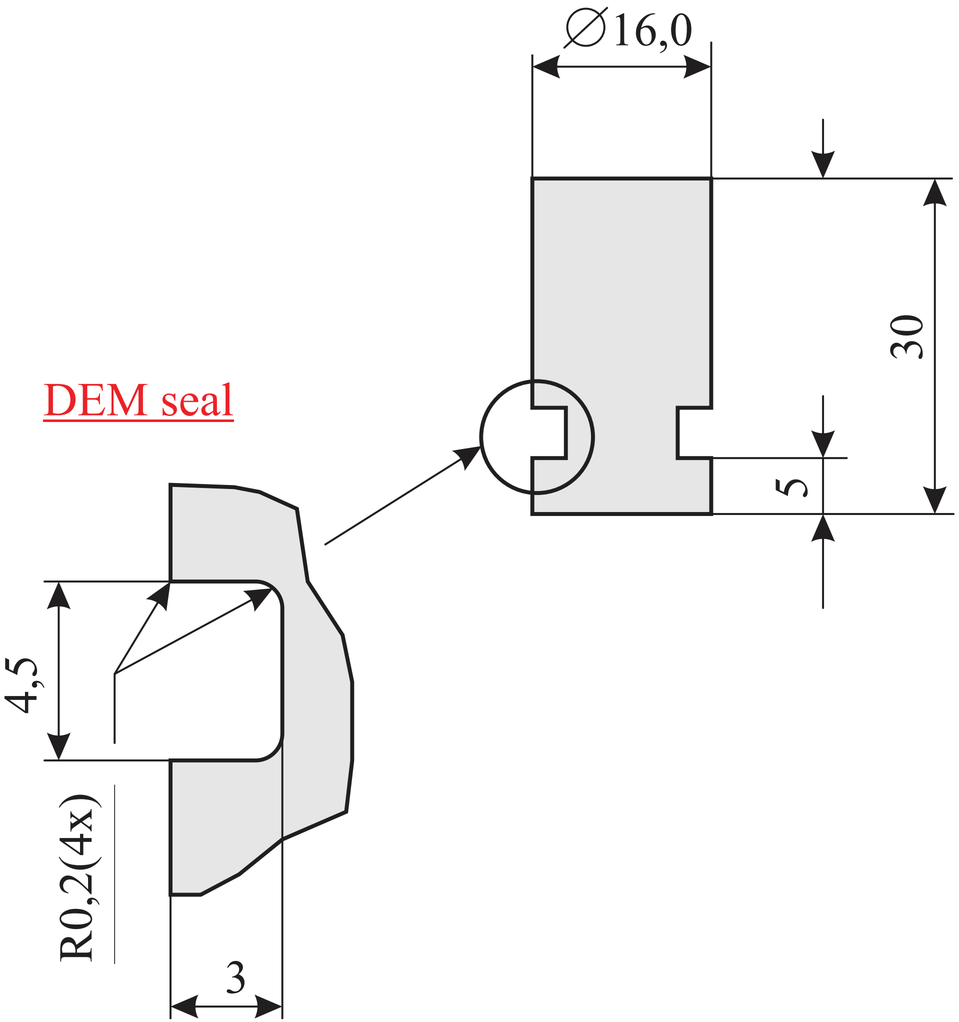

2 piston, carbon-filled teflon, 1 item

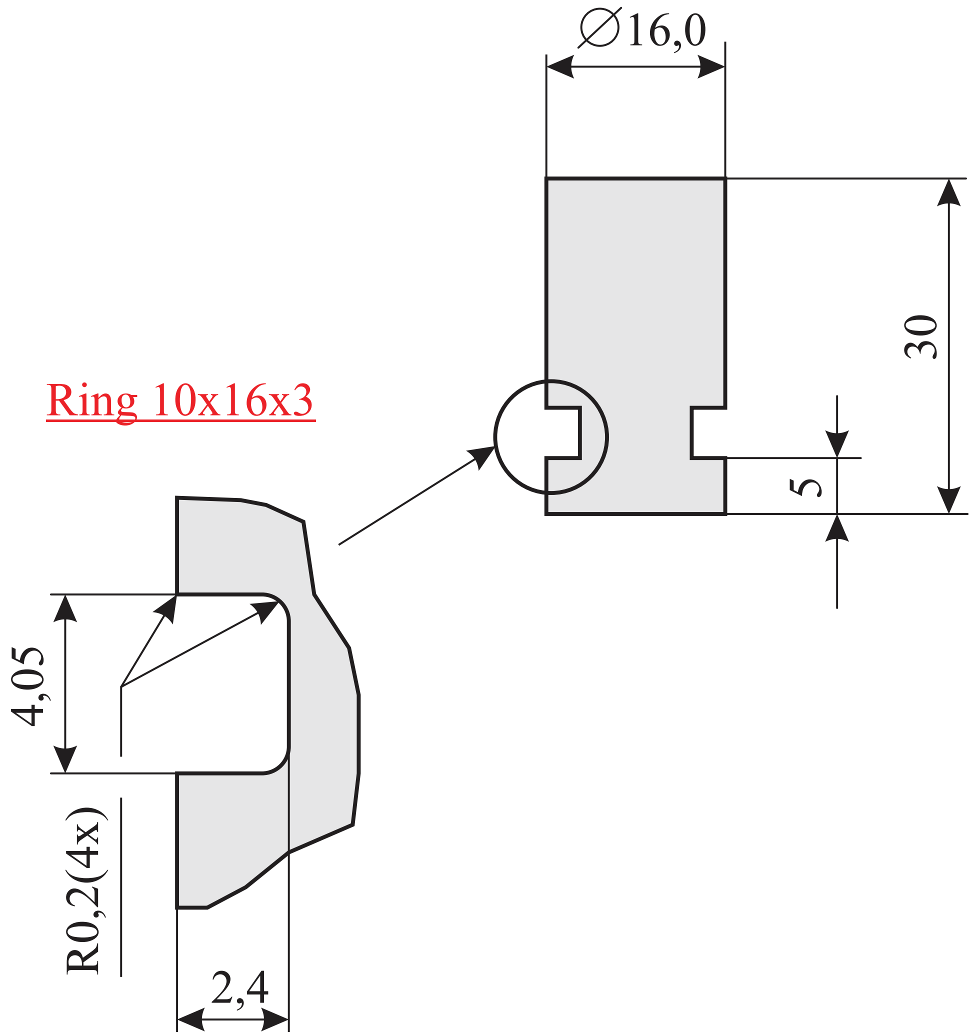

3 Cup, bronze, 1 item

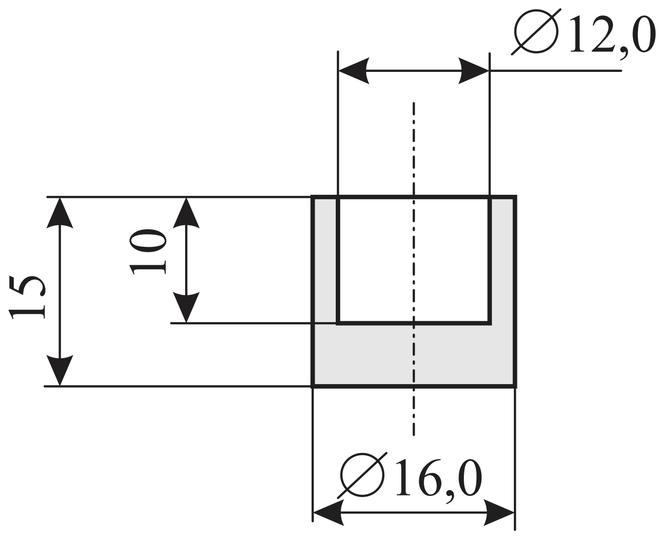

3 Cup, teflon, 1 item

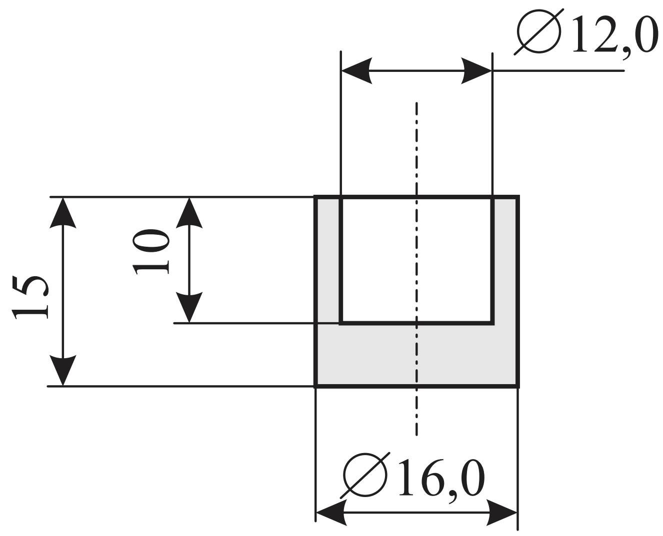

4 cylinder, steel, item

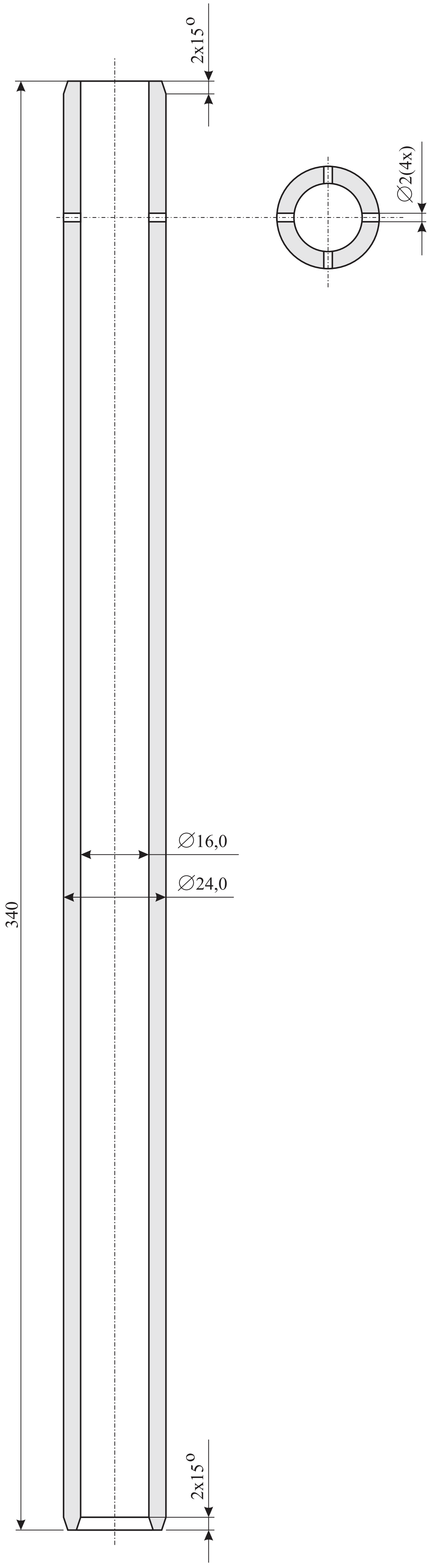

5 rod, steel, item

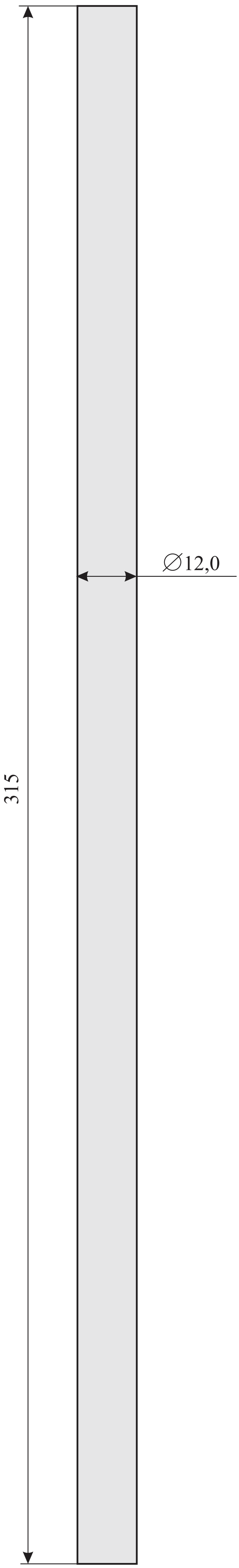

6

Connector, steel, aluminum, bronze 1 item

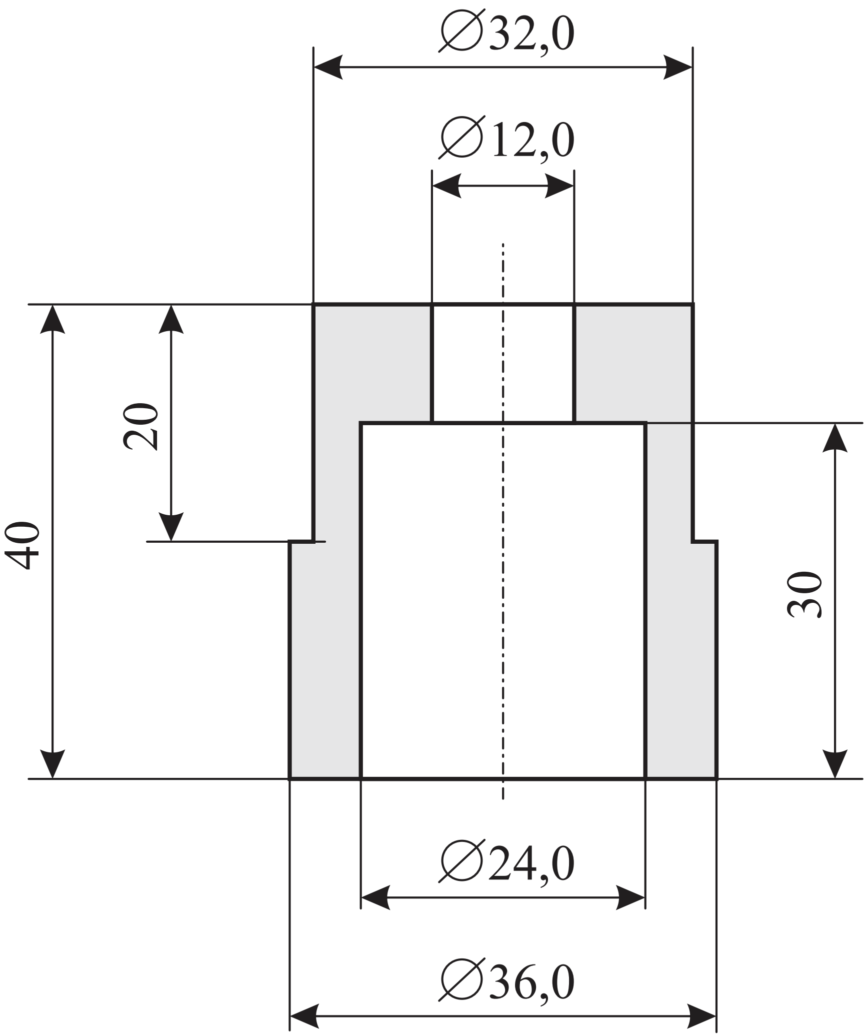

7 Upper flange, steel, bronze, aluminum,1 item

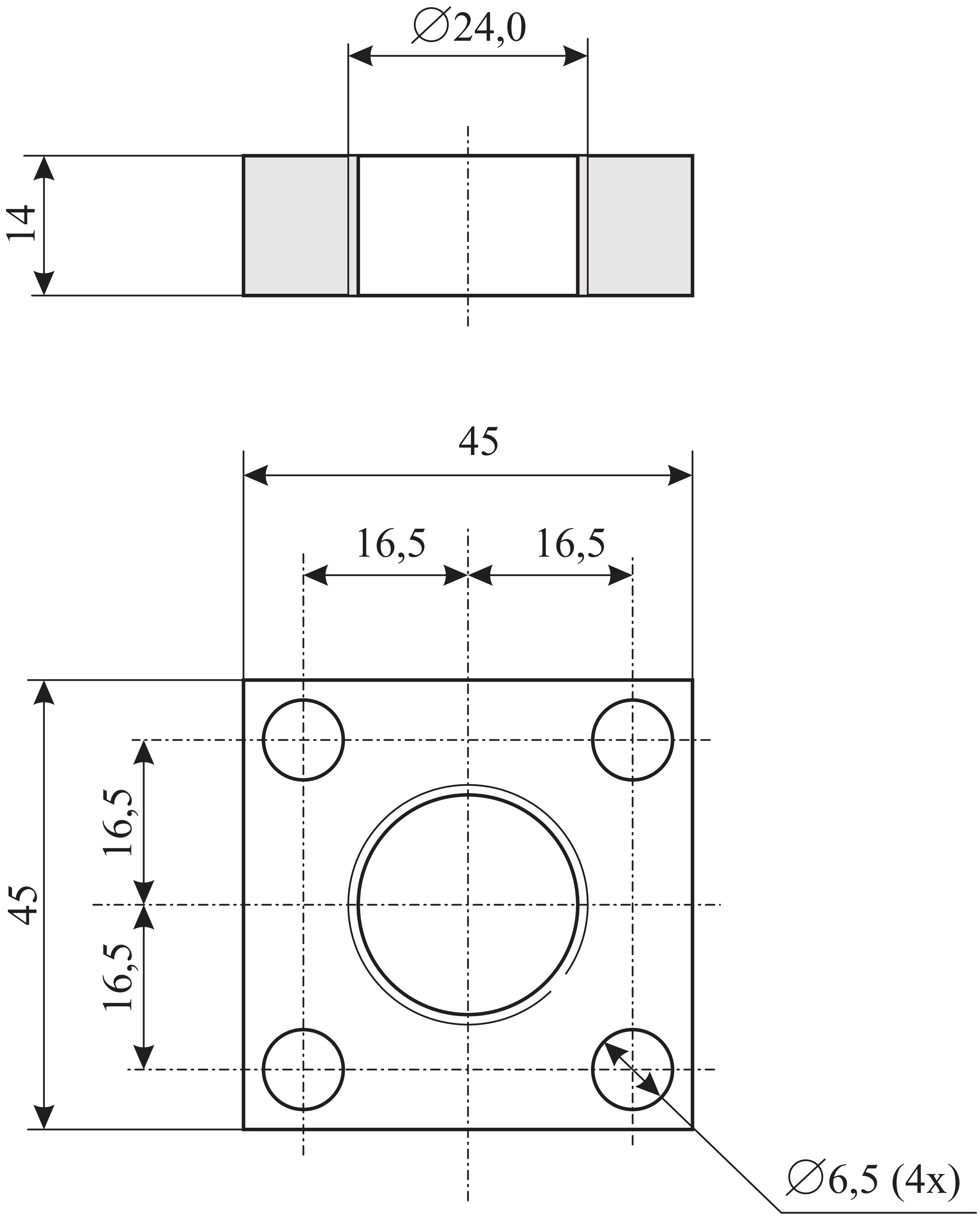

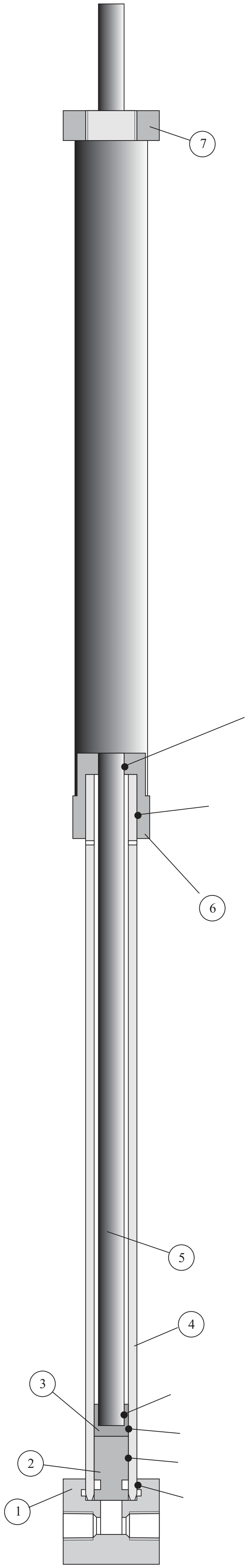
7
6
5
4
3
2
1

Annex C. Production drawings of the 40 mm indicator

1

Cover, steel, bronze 1 item

Ring 36x40x2

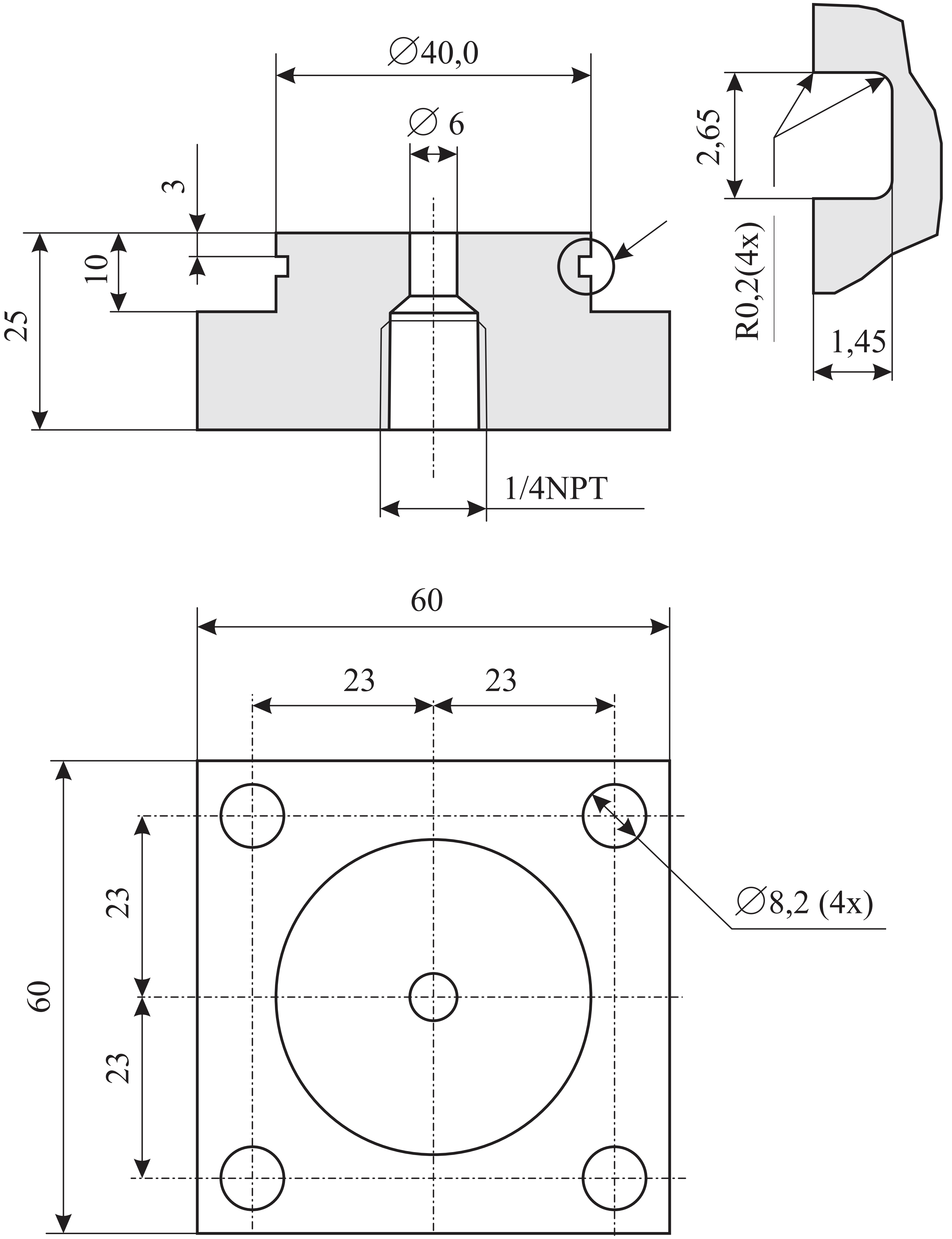

2a Piston PTFE, 2 items

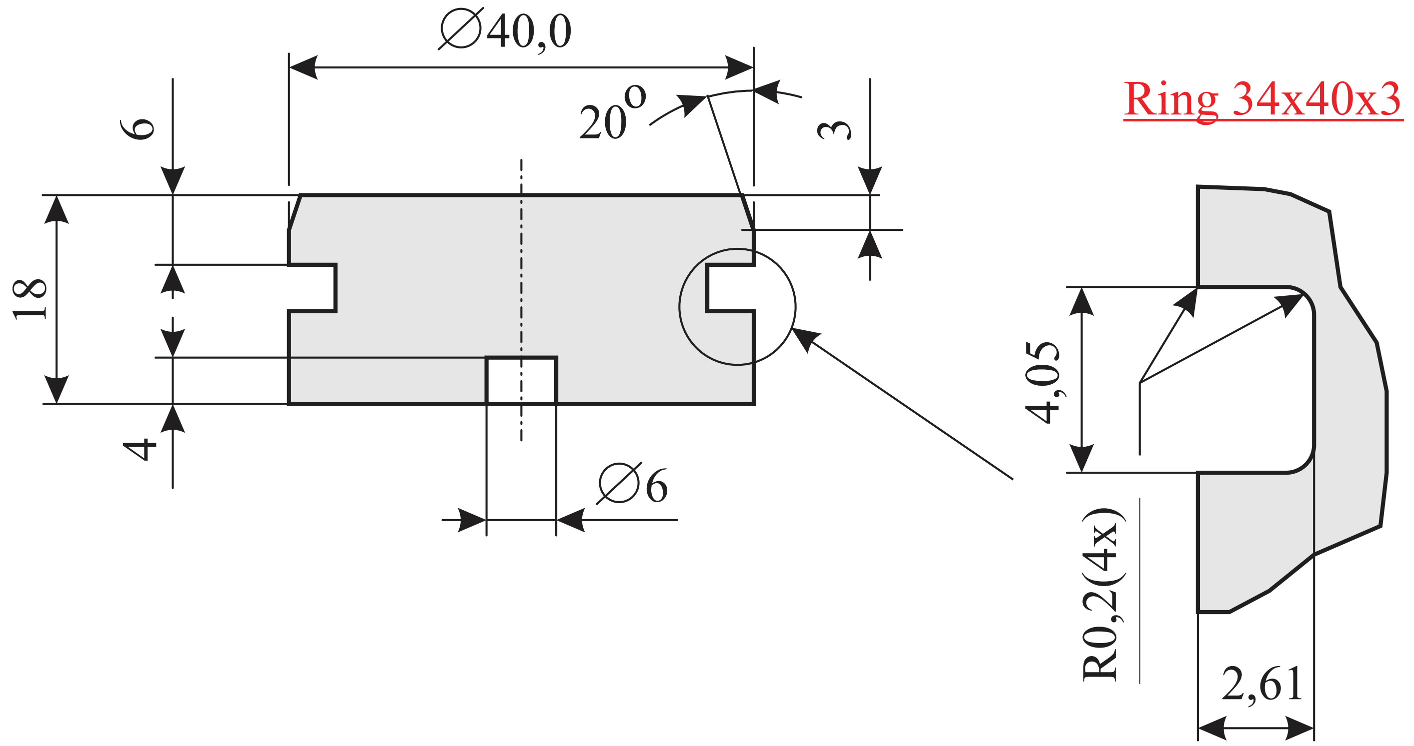

2b Piston PTFE, 2 items

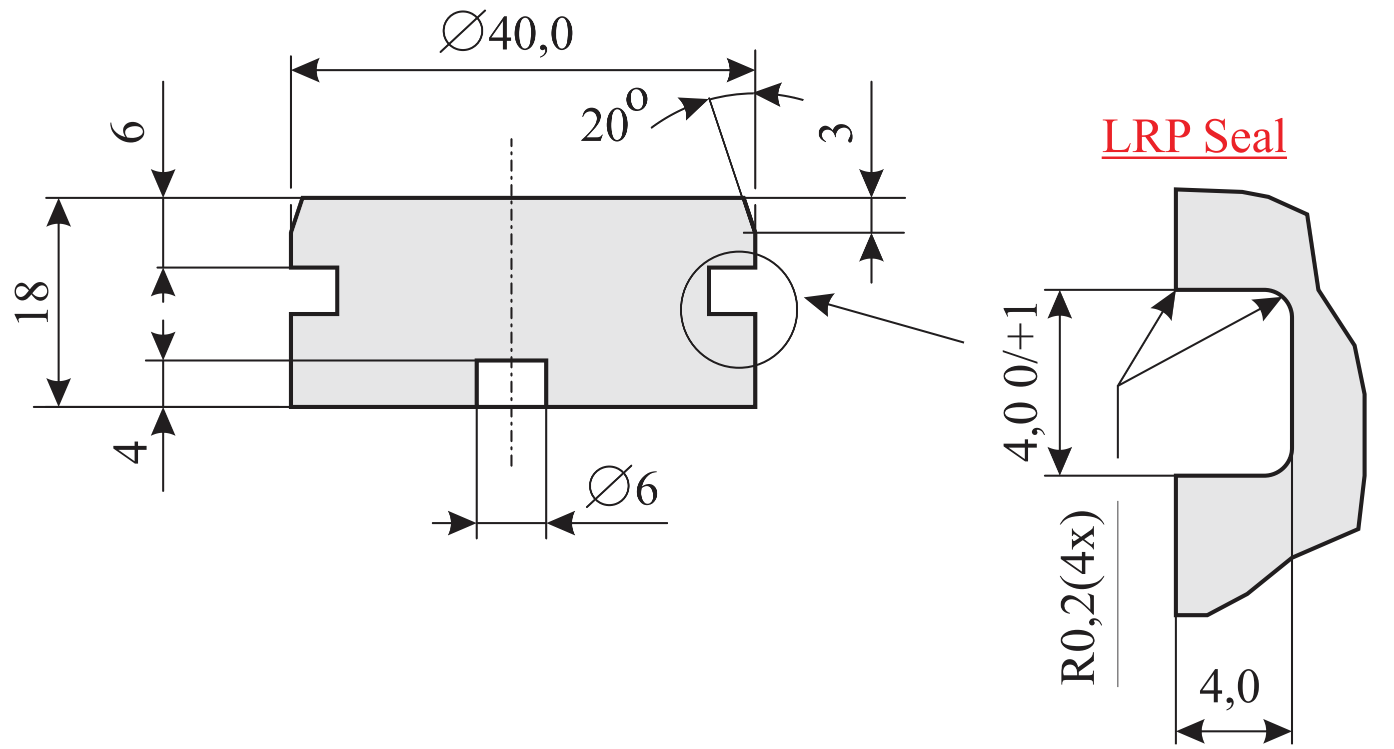

3 Rod, POM, 1 item

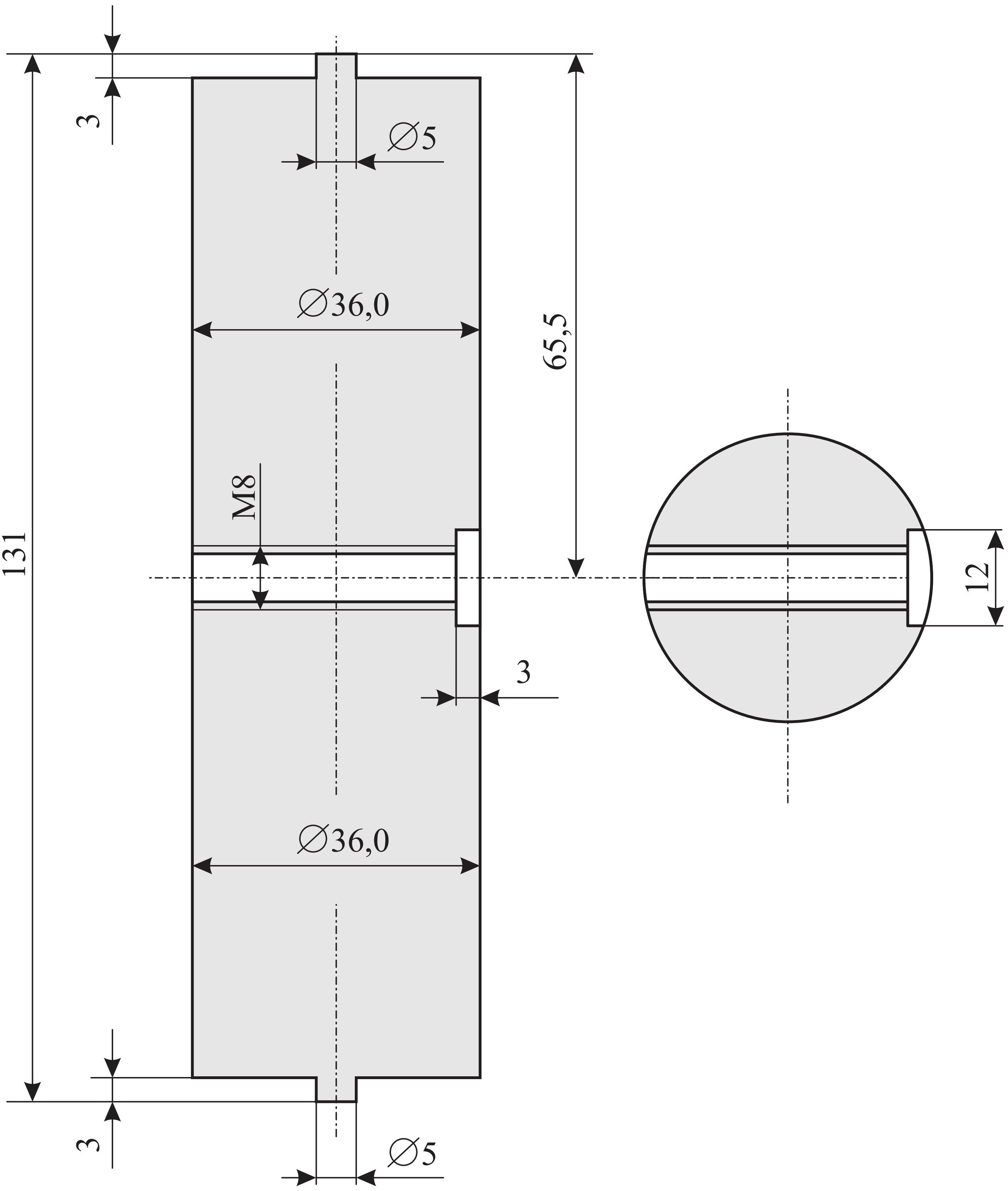

4 cylinder, steel, 2 items

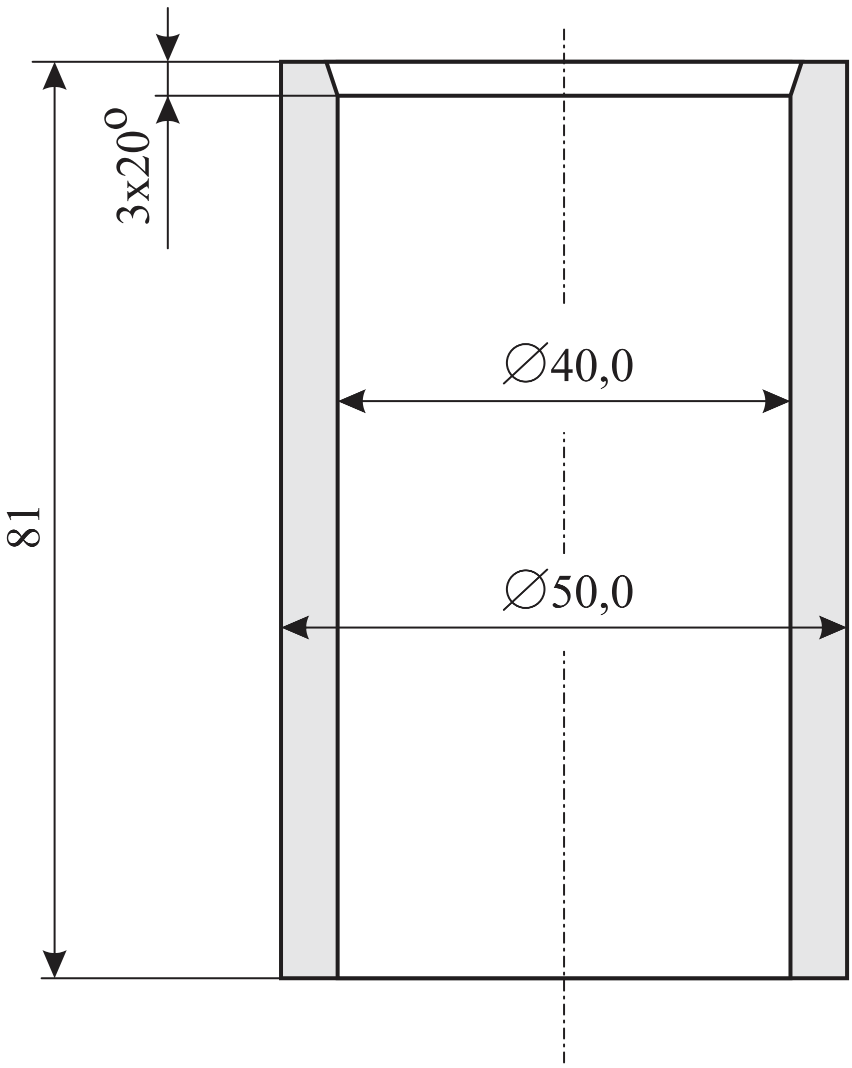

5 holder, POM, 1 item

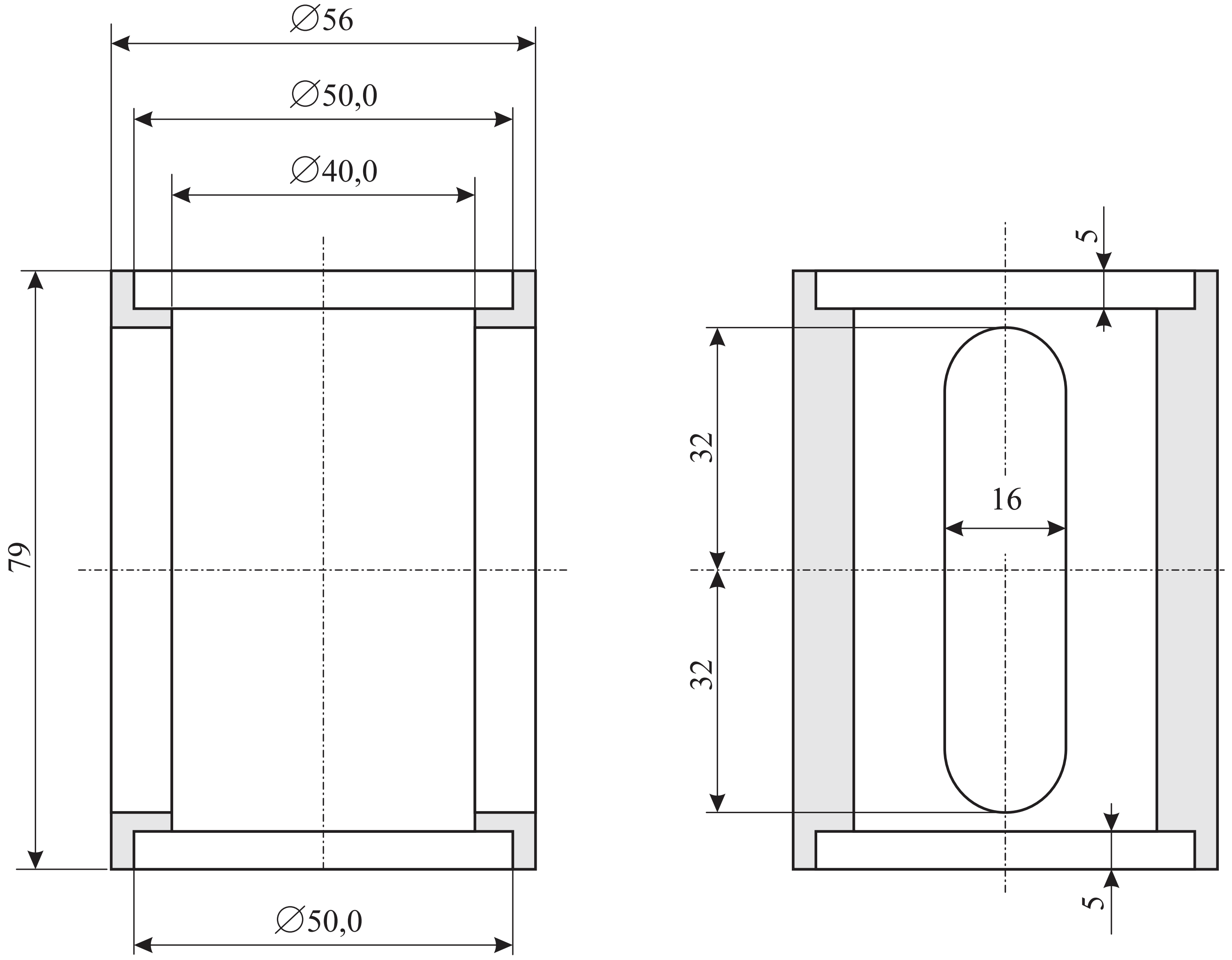

6 rod, steel, aluminum, bronze 1 item

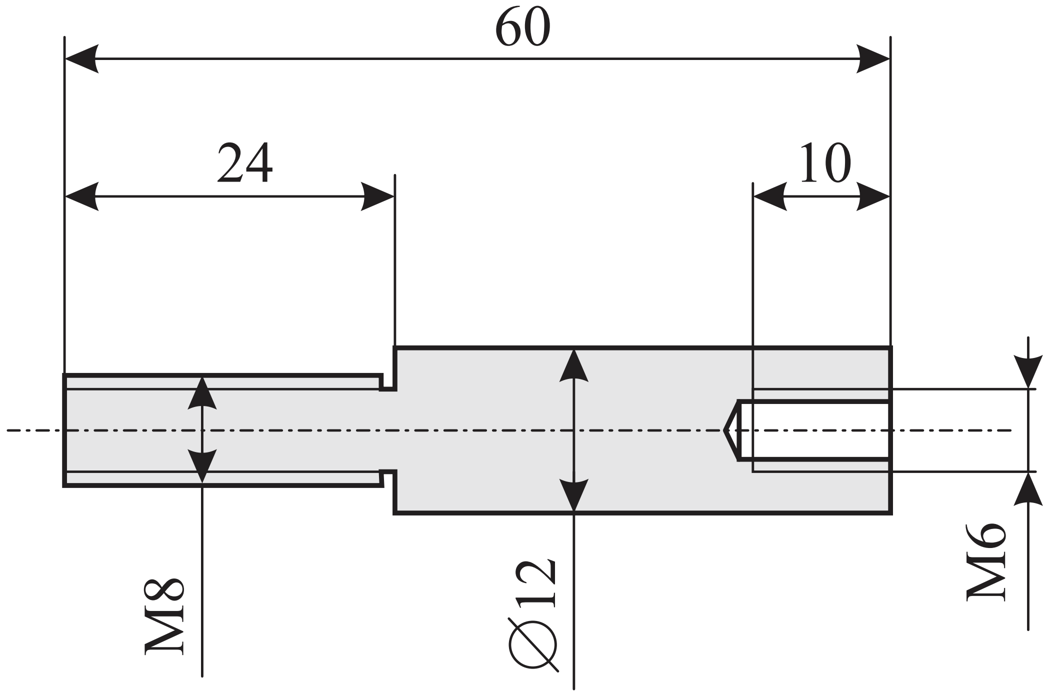

7 Cover, steel, bronze 1 item

Ring 36x40x2

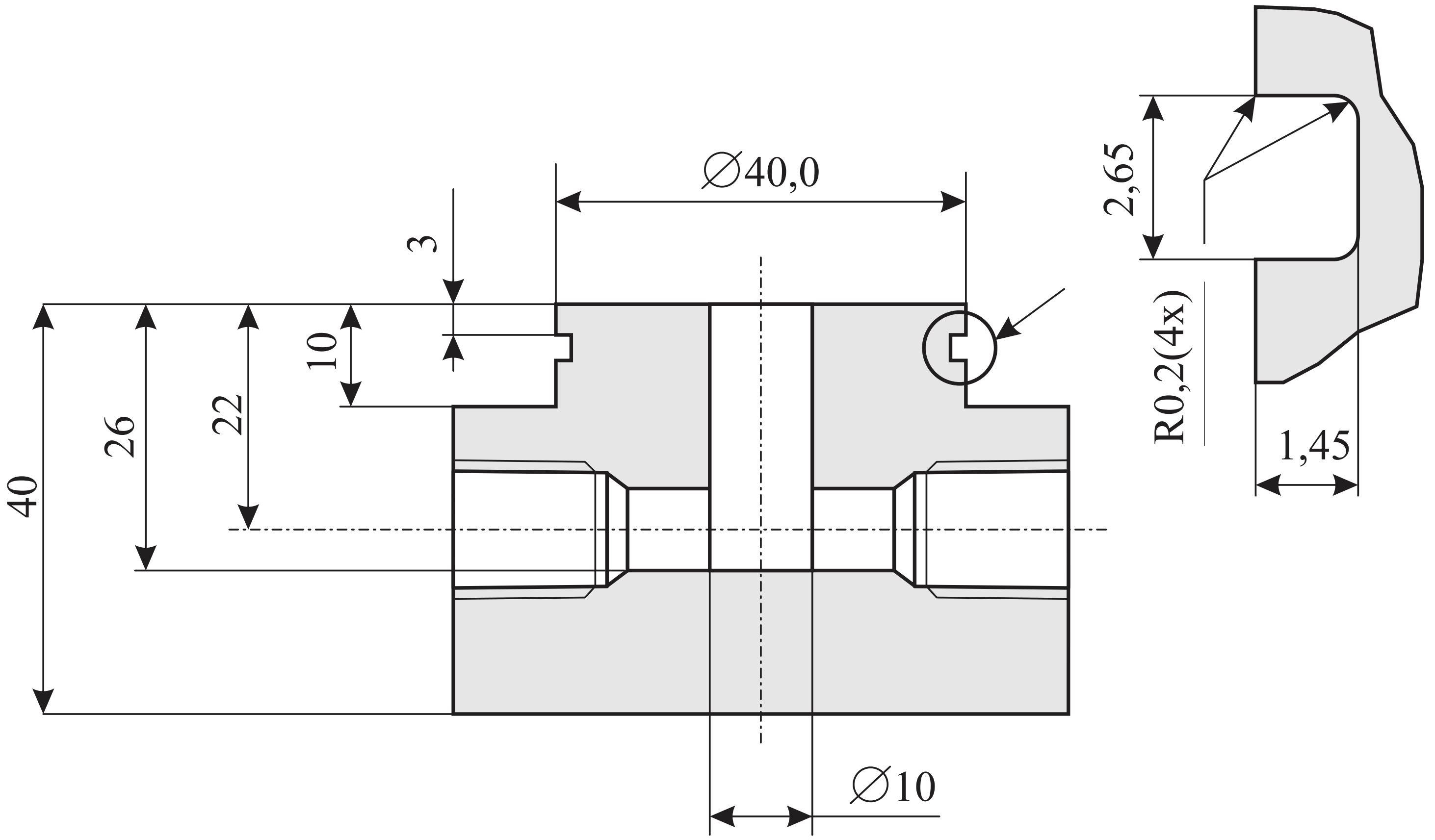

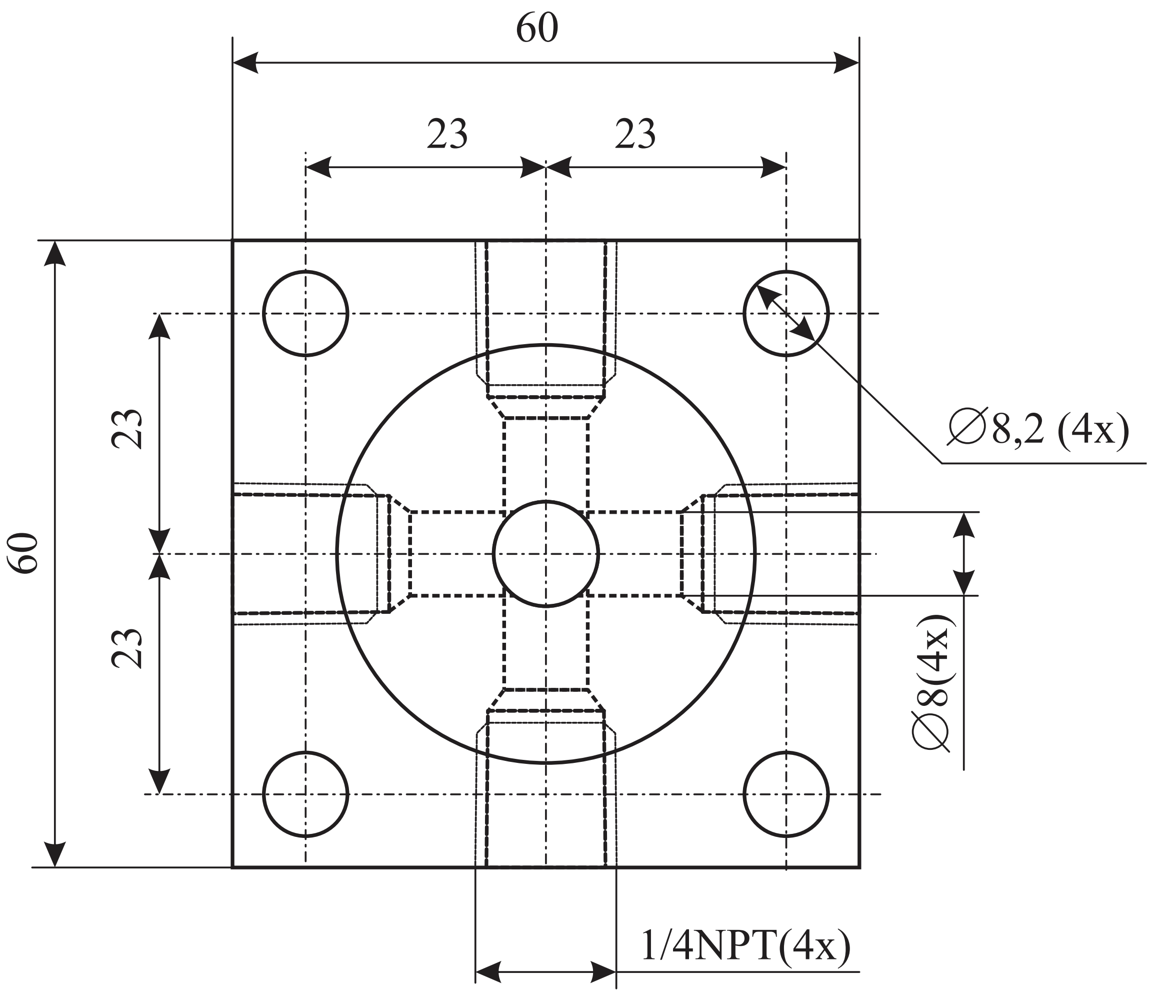

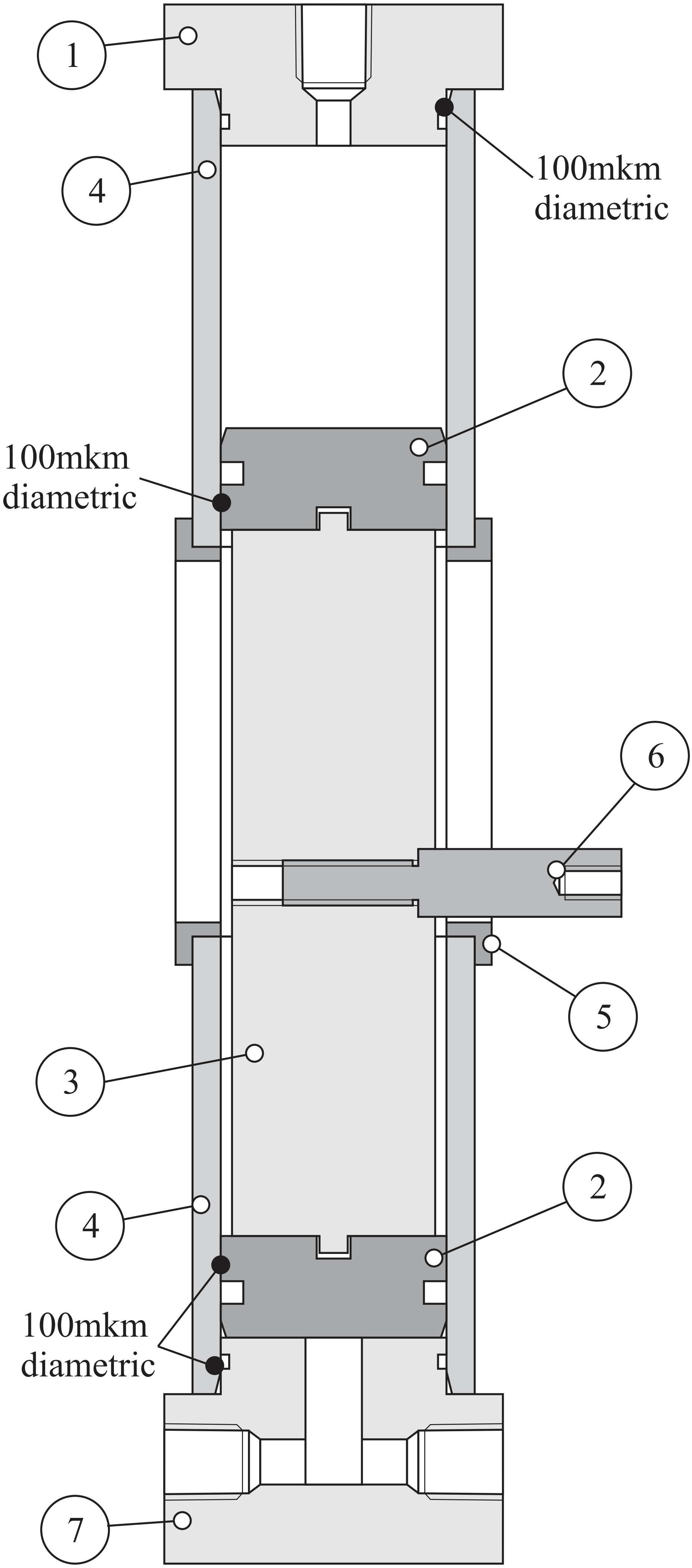

1
4
100mkm
diametric
2
100mkm
diametric
6
5
3
2
4
100mkm
diametric
7

Annex D. Sealing rings

APSOparts® the Online Shop of Angst + Pfister

APSOparts AG
Leutschenbachstrasse 55
CH-8050 Zürich
www.apsoparts.com
support@apsoparts.com

Your Product List 10.05.2019, 11:17

Quantity	Item no.	Description	Availability	Unit price	per	Price
20 pce	11.2003.0716	NORMATEC® O-ring NBR 70.00-01 ID 10.00 x 2.00 mm	Wed 15.05.2019	23.01	100pce	4.60
10 pce	11.2017.0836	NORMATEC® O-ring FKM 70.00-01 green ID 40.00 x 2.00 mm	Wed 15.05.2019	74.48	100pce	7.45
20 pce	11.2003.0748	NORMATEC® O-ring NBR 70.00-01 ID 18.00 x 2.00 mm	Wed 15.05.2019	25.34	100pce	5.07
20 pce	11.2003.0796	NORMATEC® O-ring NBR 70.00-01 ID 30.00 x 2.00 mm	Wed 15.05.2019	33.23	100pce	6.65
20 pce	11.2003.0708	NORMATEC® O-ring NBR 70.00-01 ID 8.00 x 2.00 mm	Wed 15.05.2019	23.01	100pce	4.60
10 pce	11.2017.0724	NORMATEC® O-ring FKM 70.00-01 green ID 12.00 x 2.00 mm	Wed 15.05.2019	32.03	100pce	3.20
20 pce	11.2003.0836	NORMATEC® O-ring NBR 70.00-01 ID 40.00 x 2.00 mm	Wed 15.05.2019	36.85	100pce	7.37
20 pce	11.2003.0820	NORMATEC® O-ring NBR 70.00-01 ID 36.00 x 2.00 mm	Wed 15.05.2019	36.85	100pce	7.37
5 pce	11.2003.1766	NORMATEC® O-ring NBR 70.00-01 ID 22.00 x 3.00 mm	Wed 15.05.2019	102.29	100pce	5.11
20 pce	11.2003.1776	NORMATEC® O-ring NBR 70.00-01 ID 24.00 x 3.00 mm	Wed 15.05.2019	26.95	100pce	5.39
10 pce	11.2007.0506	NORMATEC® O-ring FKM 75.00-01 ID 39.45 x 1.78 mm	Wed 15.05.2019	78.86	100pce	7.89
20 pce	11.2017.0716	NORMATEC® O-ring FKM 70.00-01 green ID 10.00 x 2.00 mm	Wed 15.05.2019	29.55	100pce	5.91
10 pce	11.2003.1882	NORMATEC® O-ring NBR 70.00-01 ID 46.00 x 3.00 mm	Wed 15.05.2019	42.39	100pce	4.24

Accuracy of prices and other information not guaranteed. This summary does not represent an actual offer. Binding prices are defined with the order confirmation. Transport will be done through DHL (parcels) and Dachser (bulk goods) our business partners for transports

APSOparts® the Online Shop of Angst+Pfister

APSOparts AG
Leutschenbachstrasse 55
CH-8050 Zürich
www.apsoparts.com
support@apsoparts.com

Your Product List 10.05.2019, 11:17

Quantity	Item no.	Description	Availability	Unit price	per	Price
10 pce	11.4006.2008	HITEC® O-ring EPDM 70.10-02 ID 8.00 x 2.00 mm	Wed 15.05.2019	40.59	100pce	4.06
10 pce	11.4006.3046	HITEC® O-ring EPDM 70.10-02 ID 46.00 x 3.00 mm	Wed 15.05.2019	78.51	100pce	7.85
5 pce	11.4006.2004	HITEC® O-ring EPDM 70.10-02 ID 4.00 x 2.00 mm	Wed 15.05.2019	211.48	100pce	10.57
20 pce	11.4006.2018	HITEC® O-ring EPDM 70.10-02 ID 18.00 x 2.00 mm	Wed 15.05.2019	48.26	100pce	9.65
10 pce	11.2007.0856	NORMATEC® O-ring FKM 75.00-01 ID 50.00 x 2.00 mm	Wed 15.05.2019	95.40	100pce	9.54
20 pce	11.4006.2012	HITEC® O-ring EPDM 70.10-02 ID 12.00 x 2.00 mm	Wed 15.05.2019	44.66	100pce	8.93
20 pce	11.4006.2010	HITEC® O-ring EPDM 70.10-02 ID 10.00 x 2.00 mm	Thu 16.05.2019	44.66	100pce	8.93
10 pce	11.4006.3024	HITEC® O-ring EPDM 70.10-02 ID 24.00 x 3.00 mm	Wed 15.05.2019	58.21	100pce	5.82
20 pce	11.4005.3024	HITEC® O-ring NBR 70.10-02 ID 24.00 x 3.00 mm	Wed 15.05.2019	37.42	100pce	7.48
10 pce	11.2007.0748	NORMATEC® O-ring FKM 75.00-01 ID 18.00 x 2.00 mm	Wed 15.05.2019	43.49	100pce	4.35

Total value of goods EUR	152.03

Accuracy of prices and other information not guaranteed. This summary does not represent an actual offer. Binding prices are defined with the order confirmation. Transport will be done through DHL (parcels) and Dachser (bulk goods) our business partners for transports